

The influence of atmospheric forcing on the interannual variability of the Adriatic mean sea level

Pupić Vurilj, Mia

Master's thesis / Diplomski rad

2022

Degree Grantor / Ustanova koja je dodijelila akademski / stručni stupanj: **University of Split, Faculty of Science / Sveučilište u Splitu, Prirodoslovno-matematički fakultet**

Permanent link / Trajna poveznica: <https://um.nsk.hr/um:nbn:hr:166:396327>

Rights / Prava: [Attribution 4.0 International](#)/[Imenovanje 4.0 međunarodna](#)

Download date / Datum preuzimanja: **2024-07-17**

Repository / Repozitorij:

[Repository of Faculty of Science](#)



UNIVERSITY OF SPLIT
FACULTY OF SCIENCE



MASTER'S THESIS

**THE INFLUENCE OF ATMOSPHERIC
FORCING ON THE INTERANNUAL
VARIABILITY OF THE ADRIATIC
MEAN SEA LEVEL**

Mia PupiĆ Vurilj

Split, September 2022

Temeljna dokumentacijska kartica

Sveučilište u Splitu
Prirodoslovno-matematički fakultet
Odjel za fiziku
Ruđera Boškovića 33, 21000 Split, Hrvatska

Diplomski rad

Utjecaj atmosferskog forsiranja na međugodišnju varijabilnost srednje razine Jadranskog mora

Mia PupiĆ Vurilj

Sveučilišni diplomski studij Fizika, smjer Fizika okoliša

Sažetak:

U ovom radu su analizirani izmjereni nizovi podataka usrednjenih razina mora kako bi se utvrdili glavni razlozi promjene razine mora zabilježene u posljednjih 50 godina. Značajni pozitivan trend, povezan s klimatskim promjenama, uočen je na svim postajama koristeći metodu najmanjih kvadrata i t-test. Koristeći Rodionov algoritam za promjenu režima pronađene su tri značajne promjene: pad razine mora 1989. od 4.37 cm koji je trajao 7 godina, porast razine mora 1996. od 2.07 cm koji je trajao 13 godina te porast razine mora 2009. od 5.3 cm koji je trajao do barem 2018. Istražena je veza srednje razine mora sa srednjim tlakom na razini mora, Sjeverno-atlantskom oscilacijom te vjetra koristeći mjesečne i godišnje podatke. Ustanovljena je značajna korelacija, ponajviše za period studeni-prosinac-siječanj-veljača. Pronađene promjene režima su analizirane provjerom sinoptičkih uvjeta. Još jednom je potvrđeno da su sve promjene režima povezane sa izraženom promjenom Sjeverno-atlantske oscilacije.

Ključne riječi: razina mora, promjena razine mora, Jadransko more, Sjeverno-atlantska oscilacija, srednji tlak na razini mora, vjetar, atmosfersko forsiranje

Rad sadrži: 43 stranice, 24 slike, 5 tablica, 14 literaturnih navoda. Izvornik je na engleskom jeziku

Mentor: prof. dr. sc. Jadranka Šepić

Ocjenjivači: prof. dr. sc. Jadranka Šepić
dr. sc. Marin Vojković
dr. sc. Iva Međugorac

Rad prihvaćen: 20. 9. 2022.

Rad je pohranjen u knjižnici Prirodoslovno-matematičkog fakulteta, Sveučilišta u Splitu.

| |
|---------------------------------|
| Basic documentation card |
|---------------------------------|

University of Split
Faculty of Science
Department of Physics
Ruđera Boškovića 33, 21000 Split, Croatia

Master's thesis

The influence of atmospheric forcing on the interannual variability of the Adriatic mean sea level

Mia Pupić Vurilj

Graduate university program Physics; specialisation: Environmental Physics

Abstract:

An analysis of the observed Adriatic mean sea-level time series has been carried out in order to determine the primary causes of the changes documented during the last 50 years. Significant positive sea-level trend, related to climate change, was detected for all stations using the least-squares method and t-test. Rodionov's regime shift index algorithm was used to detect the following three pronounced regime shifts: the 1989 shift lasting 7 years with a decrease of 4.37 cm in sea level, the 1996 shift lasting 13 years with an increase of 2.07 cm in sea level, and the 2009 shift lasting at least until 2018 with an increase of 5.3 cm in sea level. A relationship between sea-level data and North Atlantic Oscillation (NAO), mean sea-level pressure, and wind components has been explored using both monthly and yearly data and establishing significant correlation, most pronounced for the November-December-January-February (NDJF) season. Lastly, the observed regime shifts were further analysed by reviewing synoptic conditions. It was once again confirmed that all the climate shifts were related to pronounced changes of the NAO.

Keywords: Sea level, Adriatic, sea-level variability, North Atlantic Oscillation, mean sea-level pressure, wind, atmospheric forcing

Thesis consists of: 43 pages, 24 figures, 5 tables, 14 references. Original language: English

Supervisor: Prof. Dr. Jadranka Šepić

Reviewers: Prof. Dr. Jadranka Šepić
Dr. Sc. Marin Vojković
Dr. Sc. Iva Međugorac

Thesis accepted: 20.9.2022.

This thesis is deposited in the library of the Faculty of Science, University of Split.

ACKNOWLEDGEMENT

I would like to thank all of my professors for the passed-on knowledge, and in particular my thesis advisor Prof. Dr. Sc. Jadranka Šepić for her help and ample opportunities.

Also, I must express gratitude to my boyfriend, my family, and closest friends for their support during my studies and continued help. I could not have done it without them.

Contents

| | | |
|--------|--|----|
| 1. | Introduction | 1 |
| 2. | Research Context..... | 1 |
| 2.1. | The Adriatic Sea | 1 |
| 2.2. | Drivers of Sea-level Variability..... | 2 |
| 2.3. | The North Atlantic Oscillation | 3 |
| 3. | Data and Methodology | 5 |
| 3.1. | Data Sets..... | 5 |
| 3.1.1. | Sea-level Data..... | 5 |
| 3.1.2. | Climatic Data..... | 6 |
| 3.2. | Methods | 6 |
| 3.2.1. | Mean..... | 6 |
| 3.2.2. | The IB Effect and Variance | 7 |
| 3.2.3. | The Least Squares Method | 7 |
| 3.2.4. | T-Test | 8 |
| 3.2.5. | Testing Regime Shifts | 8 |
| 3.2.6. | Correlation..... | 10 |
| 4. | Results | 11 |
| 4.1. | Sea-level Analysis | 11 |
| 4.2. | Climatic Data Analysis..... | 15 |
| 4.2.1. | The North Atlantic Oscillation | 15 |
| 4.2.2. | Mean Sea-level Pressure and Wind Analysis..... | 18 |
| 4.3. | Synoptic Conditions Analysis | 24 |
| 4.3.1. | Mean Sea-level Pressure Over The Adriatic Sea..... | 30 |
| 5. | Conclusion..... | 34 |

| | |
|----------------------|----|
| Literature | 36 |
| List of Figures..... | 38 |
| List of Tables..... | 40 |
| Appendix A | 41 |
| Appendix B..... | 42 |

1. Introduction

Sea-level rise is one of major consequences of global climate change, impacting coastal and island regions around the world. Sea levels are rising and will continue to rise for centuries due to continuing deep-ocean warming and ice-sheet melt, and will remain elevated for thousands of years, even if the warming is limited. Due to the relative sea-level rise, extreme sea-level events that occurred once per century in the recent past are projected to occur at least once per year at more than half of all tide gauge locations by the year 2100 [1]. As these effects of climate change become apparent, having both socioeconomic and environmental consequences, the sea-level rise has drawn international attention. However, it is important to note that the causes of sea-level rise are not limited to those associated to the global climate change [2], as will be shown in this research.

This research aims to determine the primary causes of the sea-level variability of the Adriatic Sea documented during the last 50 years. First, a statistical analysis of yearly mean sea levels was done. Next, to explore atmospheric forcings as a possible cause of sea-level variability, relationships between the North Atlantic Oscillation (NAO), mean sea-level pressure, and wind data and sea-level data have been investigated. Additionally, sea-level time series were tested for regime shifts. Regime shifts were further analysed by reviewing governing synoptic conditions during their appearance. Results will be presented and discussed, and the conclusion will be given as a summary of the most important findings of this research.

2. Research Context

2.1. The Adriatic Sea

The area of study is the Adriatic Sea, the northernmost arm of the Mediterranean Sea, lying between the Apennine (Italian) and the Balkan Peninsula. The Adriatic Sea is about 800 km long and 200 km wide. It is divided into three basins, the Northern Adriatic, the Middle Adriatic, and the Southern Adriatic. The northern part is shallower, while the southern part is deeper, reaching about 1200 m in the South Adriatic Pit. Furthermore, the

Italian coast is smoother, without islands, whereas the eastern (mostly Croatian) coast is more indented and diverse.

Being situated at mid latitudes, the Adriatic Sea's climate is mostly Mediterranean, and the atmospheric disturbances normally propagate eastward. The summer is typically hot and dry with a dominant subtropical high-pressure zone, while the other seasons are characterized by frequent cyclones and anticyclones propagating eastward within the westerlies belt. The weather conditions are also affected by the Iceland Low and the Eurasian High in winter, and the Azores High and the Karachi Low in summer. Therefore, the air-pressure field variability over the North Atlantic, Europe, and the Mediterranean influence the cyclone activity over the Adriatic Sea [3].

Moreover, the strongest winds occur in the winter and are named bora (local 'bura') and sirocco (local 'jugo'). The bora is a cold dry katabatic wind blowing from the continental northeast with gusts reaching up to 50 m/s, causing cooling and evaporation. The sirocco, on the other hand, blows from the southeast and brings warm humid air from the Mediterranean, usually followed by the Saharan dust and rain. The bora causes coastal upwelling on the eastern coast of the Adriatic, while the sirocco is known to reverse the western coastal current and build up water in the Northern Adriatic [3]. Both winds represent transient phenomena and typically last several days. They are often coupled with migrating cyclones: when a cyclone reaches the Adriatic Sea, the sirocco wind is blowing, and when it leaves the Adriatic Sea, the bora wind event arises [4].

2.2. Drivers of Sea-level Variability

The sea-level height can be defined in two ways: the relative sea level, which is measured with respect to the surface of the solid Earth, or the geocentric sea level, which is measured with respect to a geocentric reference, such as the reference ellipsoid. The relative sea level has been measured using tide gauges during the past few centuries and estimated for longer time spans from geological records. The geocentric sea level, however, has been measured over the past few decades using satellite altimetry [5]. In this research, 'sea level' stands for the Relative Sea Level.

The global sea-level change mainly results from the thermal expansion of the ocean (thermosteric effect) and the transfer of land water to the ocean, particularly from melting

land ice (glaciers and ice sheets). However, the regional sea-level change occurs because of ocean dynamical processes, movements of the sea floor, and changes in gravity due to water mass redistribution. Therefore, at regional scales, the sea-level variability includes processes such as a dynamical redistribution of water masses and a change of water mass properties caused by changes in winds and air pressure, air–sea heat and freshwater fluxes, and ocean currents [5]. For example, the Adriatic Sea sea-level change analysis suggests that a 1 mbar increase/decrease of air pressure corresponds to a 1.8 – 2.0 cm lowering/rising of sea level, where the inverted barometer magnitude change is due to the sea level responding to other forcings (e.g. wind) as well as to air pressure [6].

Moreover, different climate variations can affect the sea level by changing the surface winds, ocean currents, temperature, and salinity. Namely, studies have shown a strong interannual and decadal variability of the Adriatic sea level, and a barotropic model driven by air pressure and wind forcing found the amplitudes for the two cycles to be less than 2 cm. According to this model, the annual cycle maximum occurs in March or April, while the interannual cycle maximum occurs in January or February and July or August. It was further discovered that the interannual sea-level variability of the Adriatic Sea correlates with the North Atlantic Oscillation (NAO), mainly through air pressure and wind alterations, and to some other processes controlling mass exchange between the Atlantic and the Mediterranean [6].

2.3. The North Atlantic Oscillation

The North Atlantic Oscillation (NAO) describes changes in the strength of two recurring pressure patterns in the atmosphere over the North Atlantic: a low near Iceland, and a high near the Azores Islands. It is an “oscillation” because the changes in atmospheric pressure are essentially an alternation between two existing patterns: a “positive phase”, in which a strong subtropical high is located over the Azores islands in the central North Atlantic while a strong low-pressure system is centred over Iceland, and a “negative phase”, in which the same pressure systems are weaker (Figure 1). The phase is determined by the NAO index, obtained from the difference of normalized sea-level pressure between stations in Iceland and the Azores (sometimes Lisbon, Portugal). Furthermore, the NAO can change its phase on a yearly basis, or the fluctuations can take place decades apart.

During winters characterized by the NAO's positive phase, high-pressure and strong low-pressure systems result in a powerful pressure gradient which in turn strengthens the westerlies bringing warmer, wetter conditions over the northern Europe and most of the northeastern North America. The Mediterranean, in contrast, experiences weaker cyclonic activity.

During winters characterized by the NAO's negative phase, the pressure systems are weaker resulting in reduced pressure gradient which weakens the pace of westerlies, causing cold, dry air to be drawn into the northern Europe from the northern Russia and the Arctic. The jet stream bypasses the weak low-pressure system over Iceland and turns south over the North Atlantic conveying moisture and warm air to the Mediterranean [7].

Because of the effects the NAO phases have over the Mediterranean, a change of its phase was suspected to be the cause of regime shifts detected in sea level.

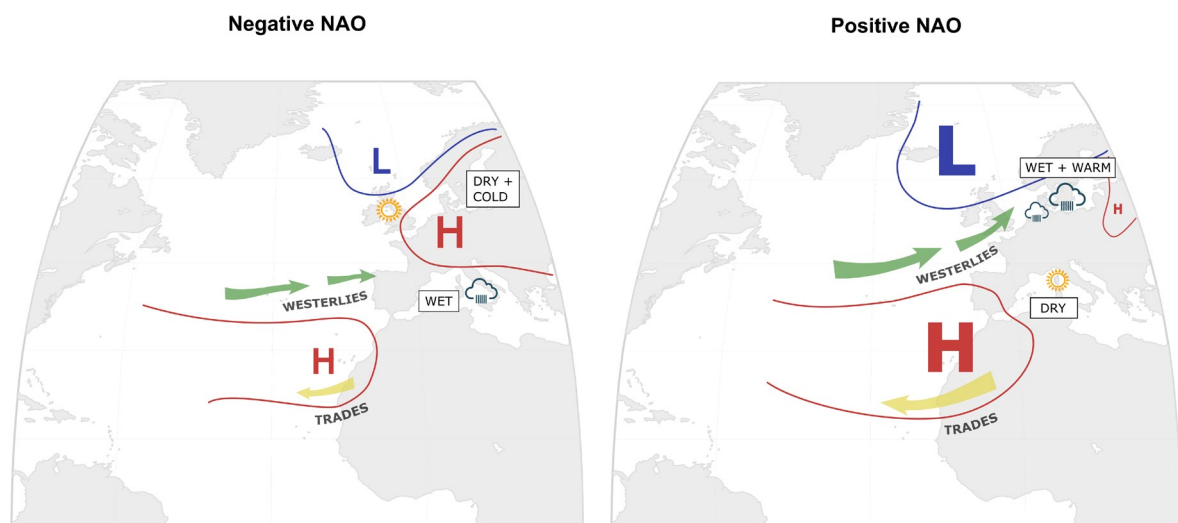


Figure 1. The negative and positive NAO phase. The strength and direction of westerlies and location of storm tracks are controlled by strength of Azores High and Iceland Low. The figure was made by the author using MATLAB R2021b and Inkscape software.

3. Data and Methodology

3.1. Data Sets

3.1.1. Sea-level Data

In order to examine the sea-level variability, monthly sea-level data were downloaded from Permanent Service for Mean Sea Level (PSMSL), the global data bank for long-term sea-level change information from tide gauges and bottom pressure recorders. The data was downloaded for seven stations located along the eastern and northern Adriatic coast: Trieste, Rovinj, Bakar, Zadar, Split, Ploče and Dubrovnik. Bakar has the longest time series, ranging from 1930 to 2020, while Ploče has the shortest, ranging from 2006 to 2018. The rest of the stations' time series range sometime from 1950s to 2018. The main downside of tide-gauge data is their poor spatial distribution and errors or gaps in the data time series. More stations would have been used if their time series were not too short, and some of the used data time series had considerable gaps, which will be further discussed later in the thesis. Station locations are shown in Figure 2.

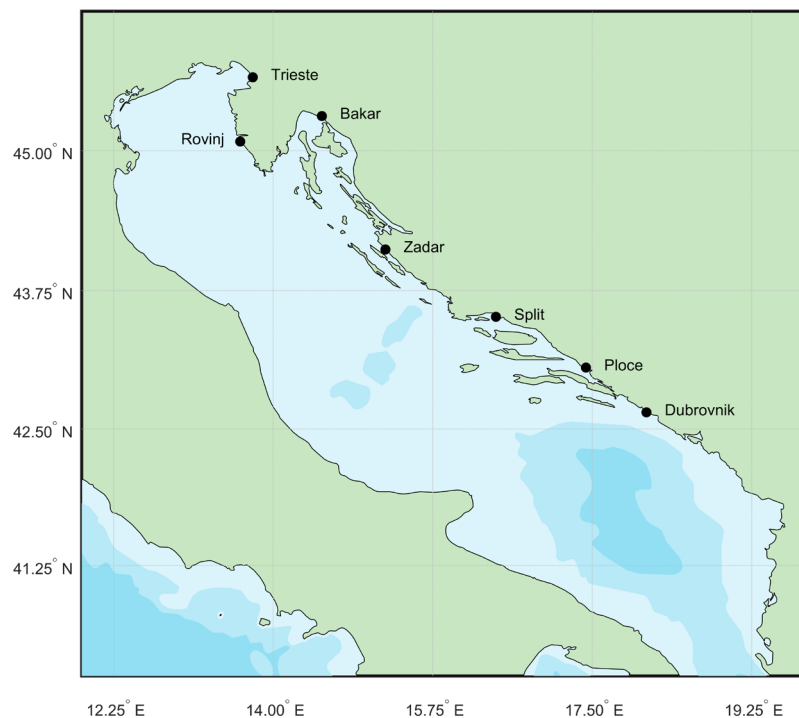


Figure 2. Location of tide gauge stations used in the study.

3.1.2. Climatic Data

The relationship between sea level and the NAO index, mean sea-level pressure, and wind data was examined. For this purpose, the monthly mean NAO index was downloaded from the National Centers for Environmental Information, National Oceanic and Atmospheric Administration (NOAA/NOAA/NOAA). This NAO index is obtained by projecting the NAO loading pattern to the daily anomaly 500 mbar height field over 0-90°N, where the NAO loading pattern has been chosen as the first mode of a Rotated Empirical Orthogonal Function (EOF) analysis using monthly mean 500 mbar height anomaly data from 1950 to 2000 over 0-90°N latitude [8]. The time series of the NAO index ranged from 1950 to 2020. Next, ERA5 monthly averaged mean sea-level pressure and 10 m wind data over the Adriatic were downloaded for a period from 1959 to 2022. These data were then calculated directly for the seven tide gauge stations. ERA5 is the fifth generation ECMWF reanalysis for the global climate and weather with a horizontal resolution of 0.25° x 0.25° (~30 km grid) for atmospheric variables [9].

Furthermore, the same ERA5 reanalysis data were used to review the synoptic conditions for years of interest, in addition to the geopotential and wind data at the 500 hPa pressure level.

3.2. Methods

This chapter gives a brief description of all methods used in this research. The analyses were entirely done using MATLAB R2021b programming software.

3.2.1. Mean

In this research, multiple types of averaging were implemented on different data sets. For each data set, the annual mean, 4-year moving mean, December-January-February-March season annual and 4-year moving mean, and November-December-January-February season annual and 4-year moving mean were estimated. Additionally, for the sea-level data the October-November-December season annual and 4-year moving mean were estimated as well. The 4-year moving mean is calculated by taking the average over a sliding window of 4 data points, moving by a year, and repeating the process.

3.2.2. The IB Effect and Variance

The inverse barometer response of sea level (η_{IB}) to surface atmospheric pressure variations was calculated using [10]:

$$\eta_{IB} = \frac{1}{g\rho_0}(\bar{p}_a - p_a) \quad (1)$$

where p_a is sea-level atmospheric pressure, \bar{p}_a is the averaged pressure over the global oceans (101325 Pa), and ρ_0 is a reference density (1028 kg/m³). Here the ERA5 mean sea-level data was used for p_a .

Next, to evaluate the agreement between the sea-level data and the calculated IB effect, with respect to both variability and magnitude, explained variance was used. The explained variance is a statistical measure of how much variation in a data set originates from a certain component. The percentage of variance of a variable y explained by another variable \hat{y} was computed using [10]:

$$var(\%) = 100 \left(1 - \frac{var(y - \hat{y})}{var(y)} \right). \quad (2)$$

3.2.3. The Least Squares Method

The least-squares method was implemented to inspect the existence of a linear trend. The least-squares method is a form of mathematical regression analysis used to determine the line of best fit for a set of data, providing a visual demonstration of the relationship between the data points [11]. This method obtains the functional dependence of measured quantities and a known independent variable. The coefficients of a linear function

$$y = ax + b + \varepsilon, \quad (3)$$

where y is a dependent measured variable, x is an independent variable, a is the slope, b is the y-intercept, and ε is the error term, are found using the following equations:

$$a = \frac{n \sum_{i=1}^n x_i y_i - \sum_{i=1}^n x_i \sum_{i=1}^n y_i}{n \sum_{i=1}^n x_i^2 - (\sum_{i=1}^n x_i)^2} \quad (4)$$

$$b = \frac{1}{n} \sum_{i=1}^n y_i - \frac{a}{n} \sum_{i=1}^n x_i. \quad (5)$$

The function and values of the function parameters are determined so that the sum of the squares of the difference between the measured and calculated values is minimal, i.e. the sum of squared error term is minimal.

3.2.4. T-Test

To determine if estimated linear trends are significant, a statistical hypothesis test, t-test, was used. The t-test follows a Student's t-distribution under the null hypothesis, which in our case states that the linear trend is insignificant.

It is possible to perform either a one-tailed or two-tailed test. In this research, a one-tailed test was performed since we are testing only one direction, a positive linear trend. The t-test produces a t-value as its result. The formula for computing the t-value for a one-tailed t-test is:

$$t = a \cdot \frac{\sqrt{\sum_{i=1}^n (x_i - \bar{x})^2}}{\sqrt{\frac{1}{n-2} \cdot \sum_{i=1}^n (y_i - \hat{y}_i)^2}}, \quad (6)$$

where, a is the least-squares function parameter, x_i the independent least-squares variable, y_i the dependent least-squares variable, \hat{y}_i the measured values, n the sample size, and $n - 2$ is the number of degrees of freedom. Once the t-value and the degrees of freedom are calculated, a p-value is determined as a statistical significance threshold (in this thesis $p = 0.05$, or 95%). If the t-value is greater than the critical value found in the table in Appendix A, then the null hypothesis is rejected in favour of the alternative hypothesis, i.e. the calculated trend is significant [12].

3.2.5. Testing Regime Shifts

The existence of regime shifts was examined using a sequential algorithm proposed by [13]. The algorithm uses a sequential t-test analysis where a number of observations come in sequence. It goes along the data set and compares each new data point with every data point in the currently existing regime. According to the t-test, the difference (*diff*) between

mean values of two subsequent regimes to be statistically significant at the level p should satisfy the condition:

$$diff = \bar{x}_2 - \bar{x}_1 = t \sqrt{\frac{2\sigma_l^2}{l}}. \quad (7)$$

Here, t is the value of the t-distribution with $2l - 2$ degrees of freedom at the given probability level p , l the cut-off parameter of the regimes to be tested, and σ_l the average variance for running l -year intervals in the time series. If a new data point deviates substantially from the regime average, it is hypothesised to be a new shift point. The existence of the new regime shift is then tested. If the shift did indeed occur, the regime shift index (RSI) is calculated as

$$RSI_{i,j} = \sum_{i=j}^{j+m} \frac{x_i^*}{l\sigma_l}, \quad m = 0, 1, \dots, l - 1, \quad (8)$$

where m is the number of years since the start of a new regime, l the cut-off parameter of the regimes to be tested, σ_l the average variance for running l -year intervals in the time series, and x_i^* the normalized deviations from the current regime average. The new shift point becomes the base point from which the test starts anew. On the other hand, if the shift did not occur, the hypothesised shift point is rejected, and the test continues as usual.

The algorithm works under the assumption of abrupt shifts and may fail for gradual transitions. The cut-off parameter, l , determines the minimum length of the regimes during which the magnitude is assumed constant. Therefore, reducing l sometimes allows detecting additional regime shifts.

This analysis was done for the annual mean sea-level data with a cut-off period of 6 years. However, to explore the existence of similar shifts for the 4-year moving mean of the NDJF season NAO index, mean sea-level pressure, and wind data, a cut-off period of 4 years was used. The p-value was always set to 0.05.

The MATLAB function used to determine the regime shifts is provided in Appendix B section of this paper. It was written following the algorithm steps provided by Rodionov that can be found in [13].

3.2.6. Correlation

The statistical Pearson correlation coefficient is a measurement of interdependence of variables. It is a value between -1 and 1 , with 1 being the strongest positive correlation, and -1 the strongest negative correlation. The positive correlation coefficient implies that the values of both variables tend to increase or decrease together, while the negative one implies that the values of one variable decrease while the other increases. In MATLAB, it is paired with a p-value which indicates the significance of the calculated correlation coefficient (in this thesis the significance threshold is set to $p = 0.05$) [14].

In this research, the correlation between sea-level data and the aforementioned climatic data was estimated.

4. Results

4.1. Sea-level Analysis

The sea-level data analysis was initiated by calculating the annual means and observing the behaviour of the sea-level time series. For easier visualisation, the annual mean sea-level anomaly was calculated as deviation from the mean sea level. It is evident that the sea-levels behave similarly for all stations (Figure 3). There are seemingly 3 distinct regimes: the first one from the 1950s to 1990, the second one from 1990 to 1995, and the third one from 1995 to present. The possible regimes, detected visually, are displayed in Figure 4, for all stations except Ploče since its time series were too short for any conclusions. The apparent difference in 1990-1995 and 2009-2018 mean values points to a possibility of a regime shift at some point.

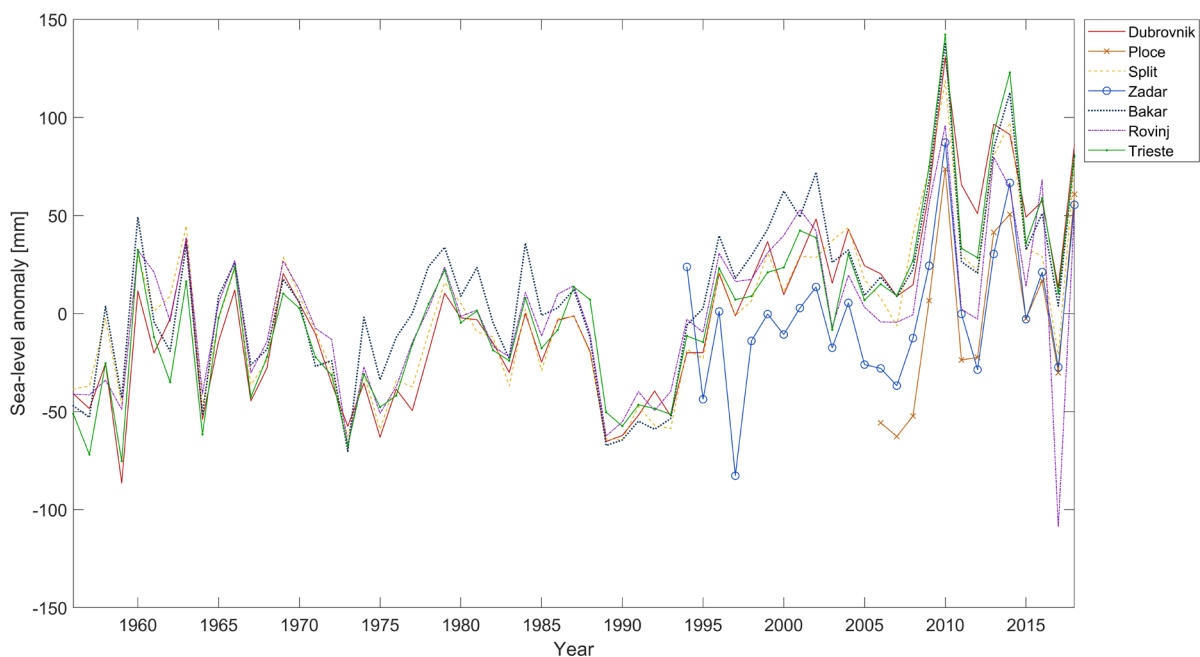


Figure 3. The annual mean sea-level anomaly for seven stations across the Adriatic coast.

Additionally, a sudden increase of sea level can be noticed in 2010, best seen for Trieste, and apparently there is a positive linear trend for all stations which have long enough data series. Furthermore, there is a sharp drop of sea level at the end of Rovinj data series, of an

unknown cause. It was more likely due to an error in the measuring device than to a year of extremely low sea levels, since this was the only year during which sea-level measured in Rovinj is significantly different than sea levels measured at other stations.

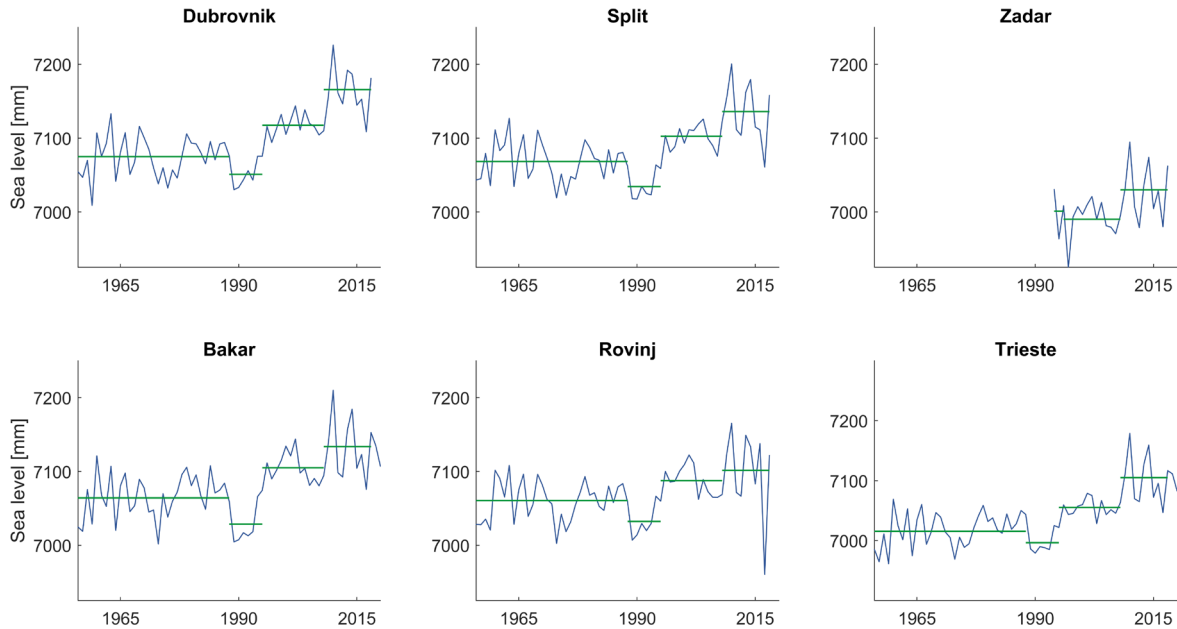


Figure 4. The annual mean sea-level data with denoted possible regimes and their means.

Now, in order to determine if there really is a positive linear trend, the least-squares method and the t-test were used. The sea-level trends differ with time and heavily depend on the length of the time series over which they are calculated. In this research the whole data series were considered when computing the trend since we were interested in possible climate change effects, i.e. sea-level rise. Positive linear trend was found and proven to be significant ($p < 0.05$) at all stations. The computed t-values, degrees of freedom, critical values from the t-distribution table (Appendix A), and the calculated trends are given in Table 1. The calculated trends show an increase of 0.7 mm/year at Rovinj, 1.03 mm/year at Split, 1.17 mm/year at Bakar, 1.47 mm/year at Trieste, 1.58 mm/year at Dubrovnik, 1.99 mm/year at Zadar, and 6.2 mm/year at Ploče station. The lowest trend (one in Rovinj) can be explained by the likely error in Rovinj measurements for 2017, while the highest trend (Ploče) is probably due to the short time series, extending only during the 21st century. The latter also points to the stronger sea-level trends in the 21st century. Linear trends are plotted in Figure 5.

Table 1. Student's t-test results.

| Station | Trend | t-value | Critical value | Degrees of freedom | Time series |
|-----------|-------------------|---------|----------------|--------------------|-------------|
| Dubrovnik | $1.58x + 3963.57$ | 6.62 | 1.670 | 61 | 1956-2018 |
| Ploče | $6.2x - 5388.74$ | 1.99 | 1.796 | 11 | 2006-2018 |
| Split | $1.03 + 5036.58$ | 4.46 | 1.669 | 63 | 1954-2018 |
| Zadar | $1.99x + 3011.47$ | 2.09 | 1.717 | 22 | 1994-2018 |
| Bakar | $1.17x + 4758.79$ | 7.02 | 1.664 | 79 | 1930-2020 |
| Rovinj | $0.7x + 5672.55$ | 2.85 | 1.670 | 61 | 1955-2018 |
| Trieste | $1.47x - 4117.26$ | 7.66 | 1.667 | 70 | 1950-2021 |

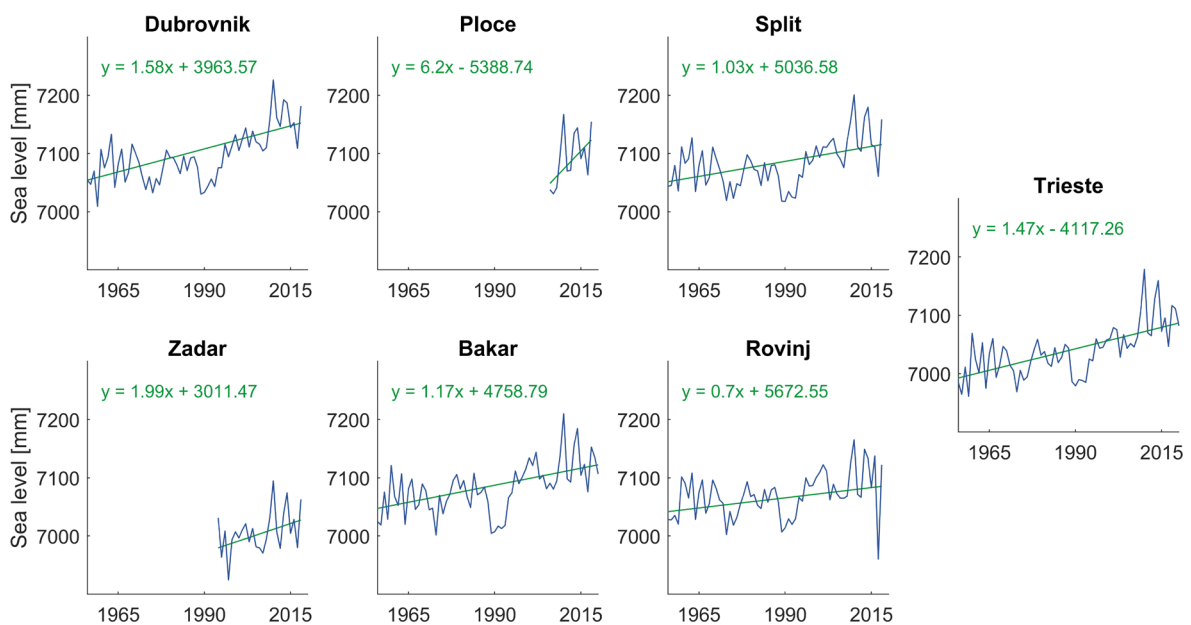


Figure 5. The annual mean sea-level data and linear trend estimated for seven stations across the Adriatic coast. Linear equations are given for each computed trend.

Next, the suspected regime shifts were examined. However, this time the analysis was done only for time series longer than 25 years (Trieste, Rovinj, Bakar, Split and Dubrovnik). The result shows that there were indeed three regime shifts: the first pronounced regime shift occurred in 1989 resulting with mean sea level lower than usual for an average of 4.37 cm during the next 7 years; the second regime shift occurred in 1996 when mean sea level increased for an average of 2.07 cm during the next 13 years; and the third regime shift, which lasted at least until 2018, started in 2009 when mean sea level abruptly increased to 5.3 cm above average during the 2009-2018 period. The deviations from the average were calculated only at the five aforementioned stations. The algorithm found some other shifts as well, but they were not constant for all stations, so they were not further analysed. All shifts are depicted in Figure 6.

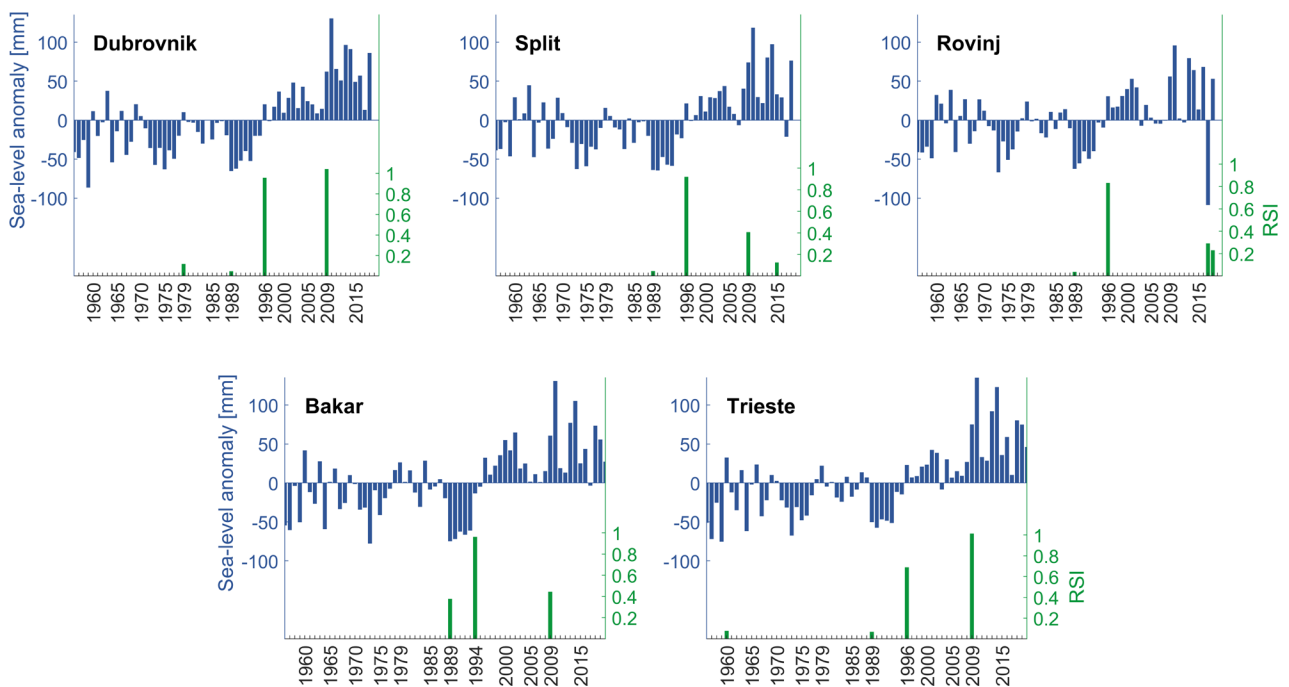


Figure 6. Regime shifts of sea levels. The upper graph displays the annual mean sea-level anomaly, while the lower graph displays the computed regime shifts. Bar plots are used for easier visualization. Three regime shifts can be detected for almost every station: in 1989, in 1996, and in 2009.

4.2. Climatic Data Analysis

4.2.1. The North Atlantic Oscillation

This section will present the results of the analysis of the impact of the NAO on the sea-level change. First, the annual means of the NAO index were calculated and then the correlation coefficient of the NAO and sea levels were found. Significant negative correlation (at $p = 0.05$) was found only for Split. However, when the analysis was done using the 4-year moving means, the results improved considerably. In this case a weak to moderate negative and statistically significant correlation was obtained for all stations, but Dubrovnik and Trieste. The results are plotted in Figure 7, and the correlation coefficients with corresponding p-values are given in Table 2 below. The plots clearly display that when the NAO is in its positive phase, the sea levels are lower than usual, and vice versa. Furthermore, the NAO phase change seen in the case of 4-year moving means evidently agrees with the sea-level regime shifts from the 1989, 1996, and 2009.

Table 2. The NAO index and sea level correlation with corresponding p-value.

| Station | Annual mean | 4-year moving mean |
|-----------|------------------------|-------------------------|
| Dubrovnik | R = - 0.19 P = 0.15 | R = - 0.23 P = 0.08 |
| Split | R = - 0.25 P = 0.05 | R = - 0.40 P = 0.001 |
| Bakar | R = - 0.23 P = 0.07 | R = - 0.29 P = 0.02 |
| Rovinj | R = - 0.23 P = 0.07 | R = - 0.37 P = 0.003 |
| Trieste | R = - 0.20 P = 0.12 | R = - 0.18 P = 0.16 |

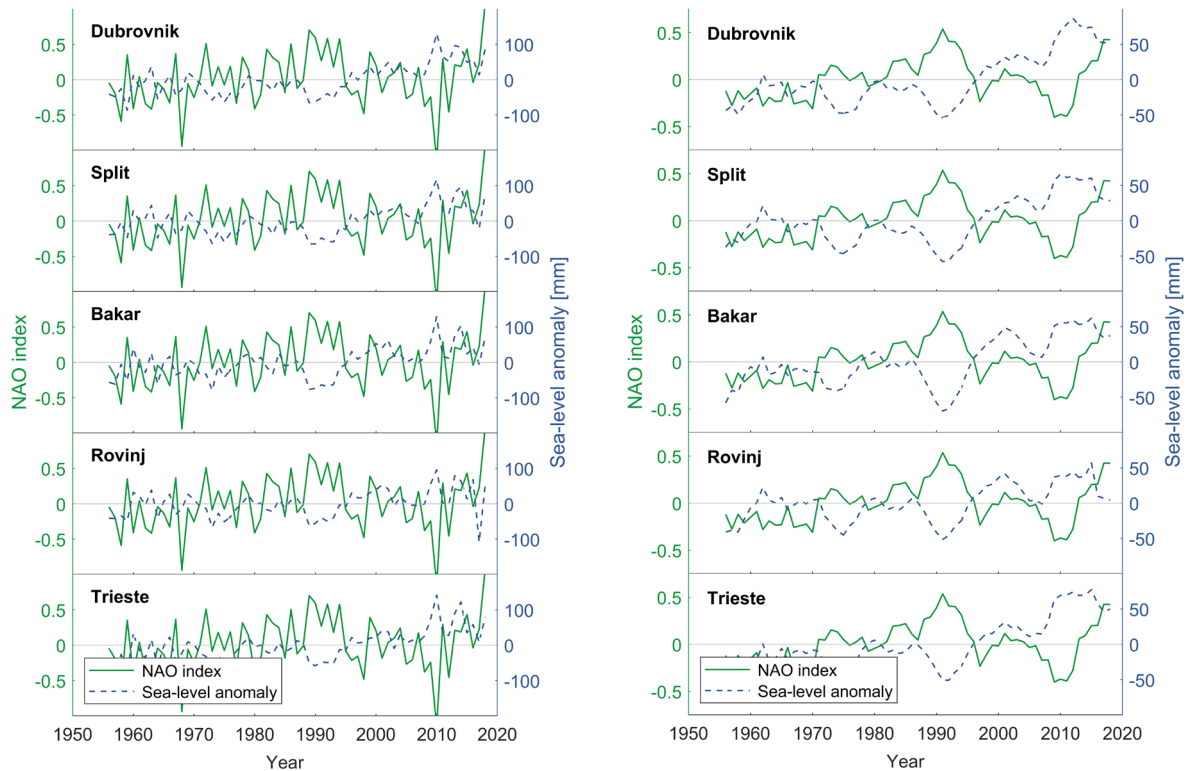


Figure 7. The NAO index and sea-level annual (left) and 4-year moving (right) means. The positive NAO index (green) corresponds to lower sea levels (dashed blue).

Moreover, since the effects of the NAO are most pronounced during the winter, the analysis was also done for monthly data. The correlation was inspected for the winter season (December, January, February, March - DJFM), fall-winter season (November, December, January, February - NDJF), and for the flood season (October, November, December - OND) sea-level annual means. Similarly as before, the analysis was repeated for the 4-year moving means, too. This time the results were the highest for the DJFM and NDJF season annual means, giving moderate negative and statistically significant correlation, with a maximum of -0.52 for Rovinj (see Table 3 for results). Since the NDJF season has slightly higher average correlation, only that season was used for further research. However, it is important to note that for the NDJF correlation analysis, the year 1991/1992 was removed from all data sets since there were no available data for Dubrovnik tide gauge. The NDJF season and sea-level data annual means are presented in Figure 8, with missing data evident for Dubrovnik. Negative correlation between the two data sets is evident.

Table 3. The NAO index and sea level correlation with p-value for the DJFM and NDJF season.

| Station | DJFM | NDJF | DJFM 4y | NDJF 4y |
|-----------|--|--|-------------------------|--|
| Dubrovnik | R = - 0.42 P = $7.92 \cdot 10^{-4}$ | R = - 0.39 P = 0.0019 | R = - 0.23 P = 0.07 | R = - 0.22 P = 0.09 |
| Split | R = - 0.51 P = $2.34 \cdot 10^{-5}$ | R = - 0.5 P = $4.08 \cdot 10^{-5}$ | R = - 0.41 P = 0.001 | R = - 0.42 P = $7.95 \cdot 10^{-4}$ |
| Bakar | R = - 0.43 P = $5.23 \cdot 10^{-4}$ | R = - 0.46 P = $1.69 \cdot 10^{-4}$ | R = - 0.29 P = 0.02 | R = - 0.32 P = 0.01 |
| Rovinj | R = - 0.38 P = 0.0023 | R = - 0.52 P = $1.71 \cdot 10^{-5}$ | R = - 0.24 P = 0.06 | R = - 0.46 P = $1.69 \cdot 10^{-4}$ |
| Trieste | R = - 0.37 P = 0.0028 | R = - 0.40 P = 0.0015 | R = - 0.16 P = 0.21 | R = - 0.21 P = 0.11 |

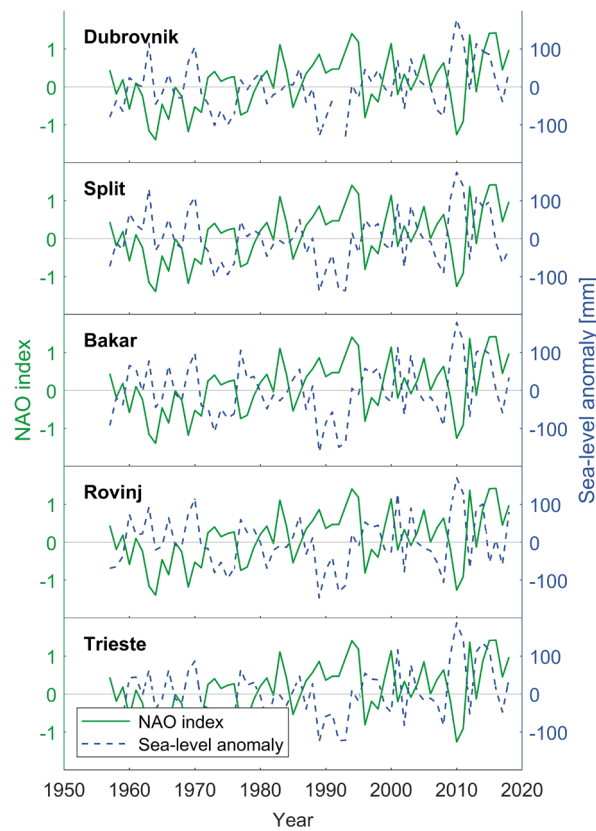


Figure 8. The NAO index and sea level Nov-Dec-Jan-Feb season annual means. The positive NAO index (green) corresponds to lower sea levels (dashed blue).

Since the NAO phase change agrees with the sea-level regime shifts from the 1989, 1996, and 2009, the regime shifts were further evaluated. The review of the 4-year moving mean NAO regime shifts indeed resulted with, among others, the three shifts of interest: 1989, 1995 (associated to the 1996 shift), and 2009, as presented on the left panel of Figure 9. A strong regime shift was found in 2013 when the NAO phase became positive once again. The regime shifts were evaluated for the NDJF season as well, using the 4-year moving mean. This time the 1996 and 2008 (2009) shifts were detected, but not the 1989 shift, which was found only for the complete NAO annual analysis (Figure 9, right). Again, the latest regime shift was detected for the positive NAO phase, here in 2012.

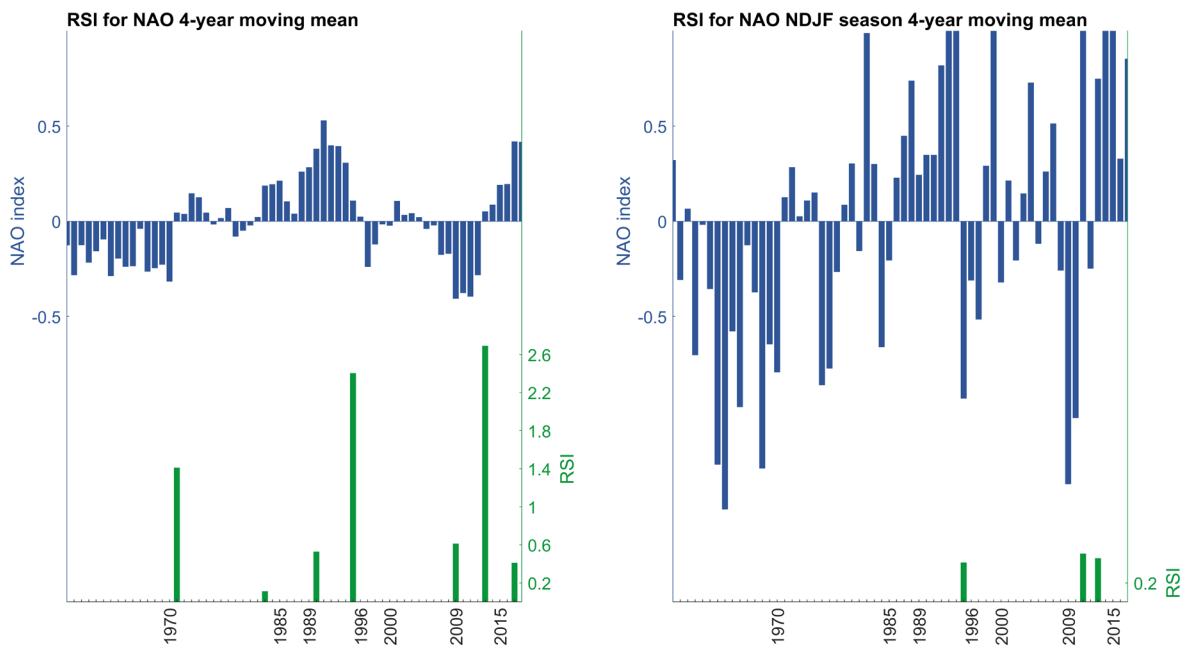


Figure 9. The NAO index regime shifts in case of a 4-year moving mean (left) and Nov-Dec-Jan-Feb season 4-year moving mean (right). Multiple regime shifts were detected, including the shifts around the years of interest: 1989, 1996, and 2009.

4.2.2. Mean Sea-level Pressure and Wind Analysis

The inverse barometer effect was suspected to be one of the reasons for the sea-level change since the NAO index corresponds to the difference between the Icelandic Low and the Azores High sea-level pressure systems. Hence, the correlation between the mean sea-level pressure and sea-level data was calculated. Here the NDJF season annual means and

4-year moving means were used for both types of data. As expected, high and significant correlation between the two was established (Table 4). This is evident from the plot displayed in Figure 10. Clearly, the two series closely follow each other.

Table 4. Mean sea-level pressure and sea-level data NDJF season annual and 4-year moving mean correlation with corresponding p-value.

| Station | NDJF | NDJF 4y |
|-----------|---|---|
| Dubrovnik | R = - 0.84 P = $3.14 \cdot 10^{-11}$ | R = - 0.78 P = $9.75 \cdot 10^{-9}$ |
| Split | R = - 0.86 P = $4.69 \cdot 10^{-12}$ | R = - 0.84 P = $4.14 \cdot 10^{-11}$ |
| Bakar | R = - 0.89 P = $6.95 \cdot 10^{-14}$ | R = - 0.85 P = $1.37 \cdot 10^{-11}$ |
| Rovinj | R = - 0.87 P = $2.34 \cdot 10^{-12}$ | R = - 0.84 P = $3.03 \cdot 10^{-11}$ |
| Trieste | R = - 0.87 P = $1.88 \cdot 10^{-12}$ | R = - 0.82 P = $4.64 \cdot 10^{-10}$ |

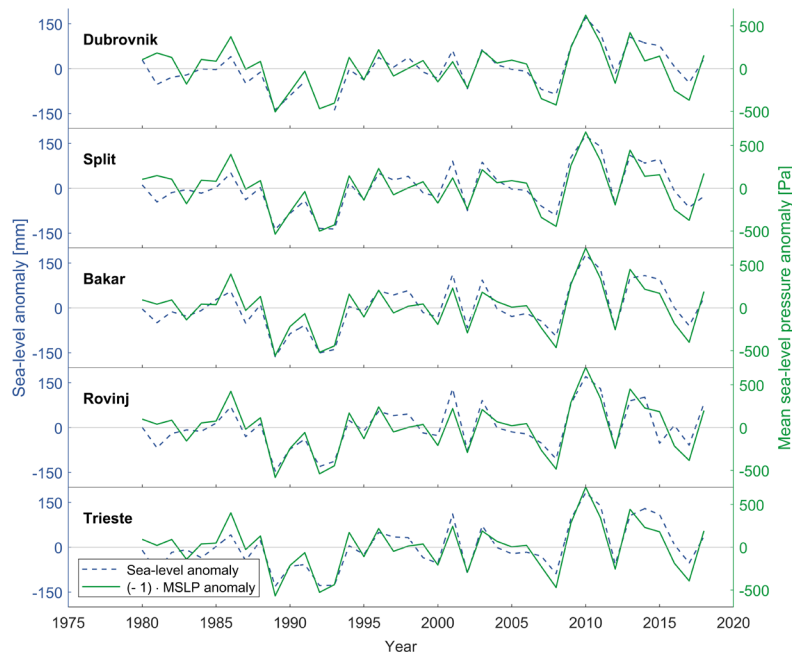


Figure 10. Sea level (dashed blue) and mean sea-level pressure anomaly (green) NDJF season annual means. The mean sea-level pressure data was multiplied by -1 for easier interpretation of correlation.

However, simply plotting the mean sea-level pressure data does not account for the IB effect's magnitude when compared to the sea-level data. Equation (1) was used to account for both the magnitude and variability of the IB effect, while the explained variance (2) was used to quantify its contribution to the observed sea-level variability. The 4-year moving mean of sea-level and IB effect data were used, first for the complete data series, then only for the NDJF season. The computed variance ranges from 18.7% at Dubrovnik to 30.7% at Rovinj, for the complete time series, and from 40.4% at Dubrovnik to 49% at Rovinj for the NDJF season time series. Therefore, the sea-level variability is explained only partially by the IB effect, but almost up to a half for the NDJF season. The results are displayed in Figure 11. Additionally, the mean sea-level pressure regime shifts were detected for 1989, 1995, and 2010. Another regime shift was found for 2016 (Figure 12). This evidently agrees with the sea-level and the NAO regime shifts.

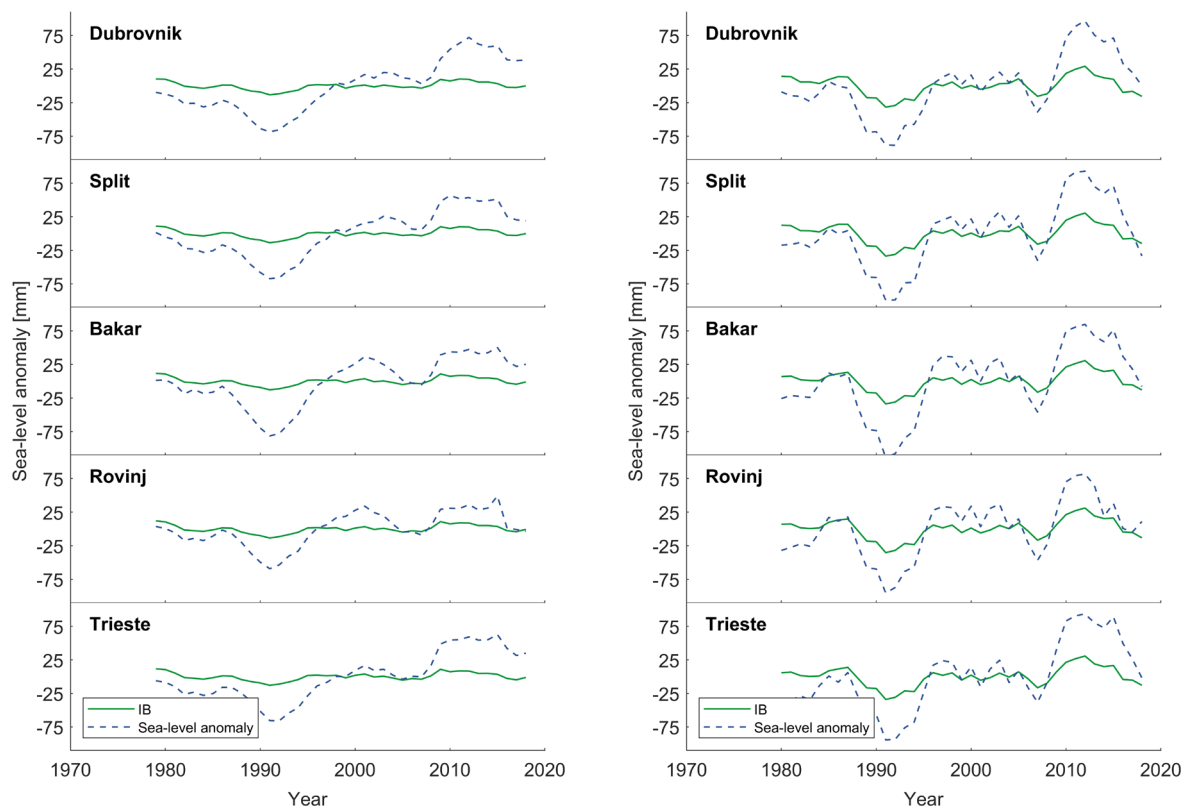


Figure 11. Sea-level anomaly and the IB effect of the complete data set (left) and the NDJF season (right). Both time series were smoothed using a 4-year moving mean.

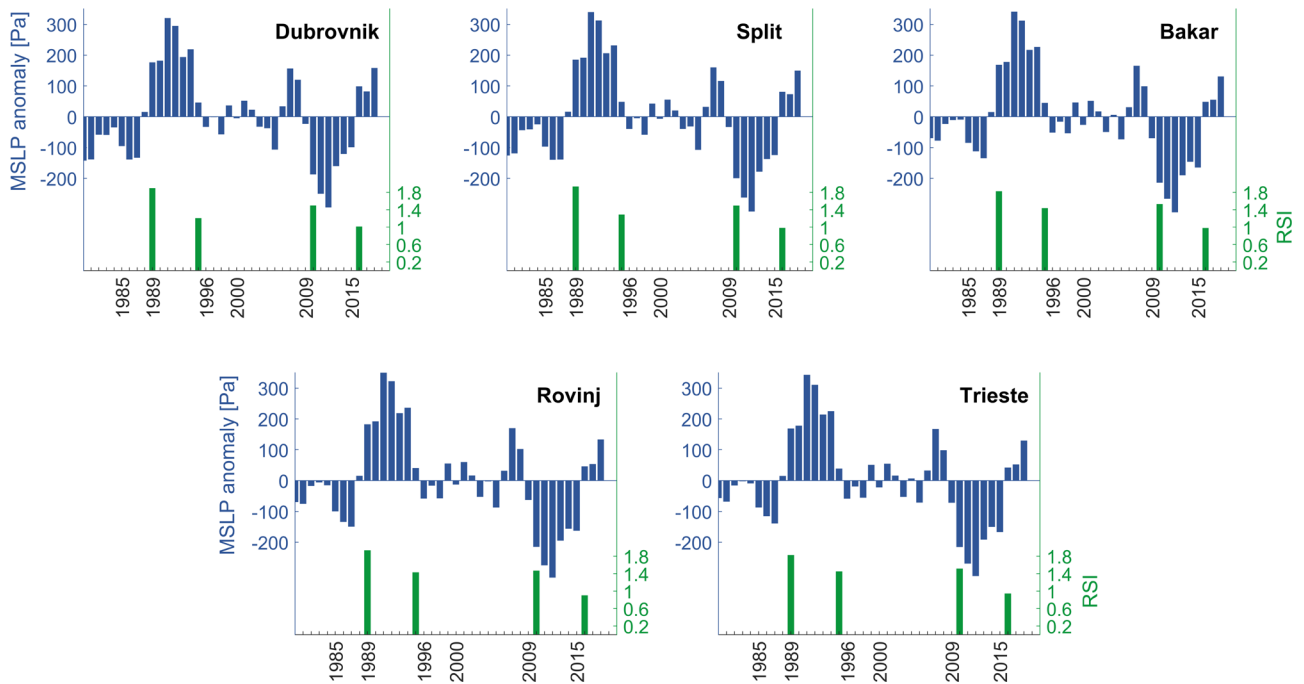


Figure 12. Mean sea-level pressure regime shifts for the NDJF season. The shifts were calculated for 4-year moving mean dataset. Four regime shifts can be detected for all data: in 1989, 1995, 2010, and in 2016.

Next, since the NAO influences the strength and direction of westerlies, wind field data analysis was done. The correlation was calculated for two wind components: a component parallel to the Adriatic, and a component orthogonal to the Adriatic. The parallel component has a north-westward positive direction, while the orthogonal component has a north-eastward positive direction. High to moderate and statistically significant correlation was obtained for the parallel component, while the orthogonal component proved to be less correlated, as seen from Table 5. The result is displayed in Figure 13, from which it can be observed that the orthogonal component's variability is not as similar to the sea-level variability as the parallel component's is. This is presumably because of the downwelling, and upwelling caused by the Ekman transport for which the wind has to be parallel to the coast, and additionally because of the piling up of water caused by the sirocco wind. Further analysis of the variance is needed to quantify the wind contribution to the observed sea-level variability, which was not in the scope of this research. Again, the regime shift analysis was done, establishing multiple regime shifts for the parallel component, including the shifts in 1989 (1988), 1995, and 2009 for some stations (Figure 14). For the orthogonal component, on the other hand, fewer shifts were found, but they included the shifts around 1989 and 2009 for all stations (Figure 15).

Table 5. Correlation coefficients and its p-value for the parallel (\parallel) wind component and the orthogonal (\perp) wind component and sea-level data. The NDJF season annual means were used.

| Station | \parallel component | \perp component |
|-----------|---------------------------------------|--|
| Dubrovnik | R = 0.84 P = $8.14 \cdot 10^{-11}$ | R = - 0.60 P = $6.09 \cdot 10^{-5}$ |
| Split | R = 0.79 P = $3.59 \cdot 10^{-9}$ | R = - 0.22 P = 0.19 |
| Bakar | R = 0.62 P = $3.12 \cdot 10^{-5}$ | R = - 0.09 P = 0.61 |
| Rovinj | R = 0.51 P = 0.0011 | R = - 0.09 P = 0.58 |
| Trieste | R = 0.60 P = $6.19 \cdot 10^{-5}$ | R = - 0.07 P = 0.69 |

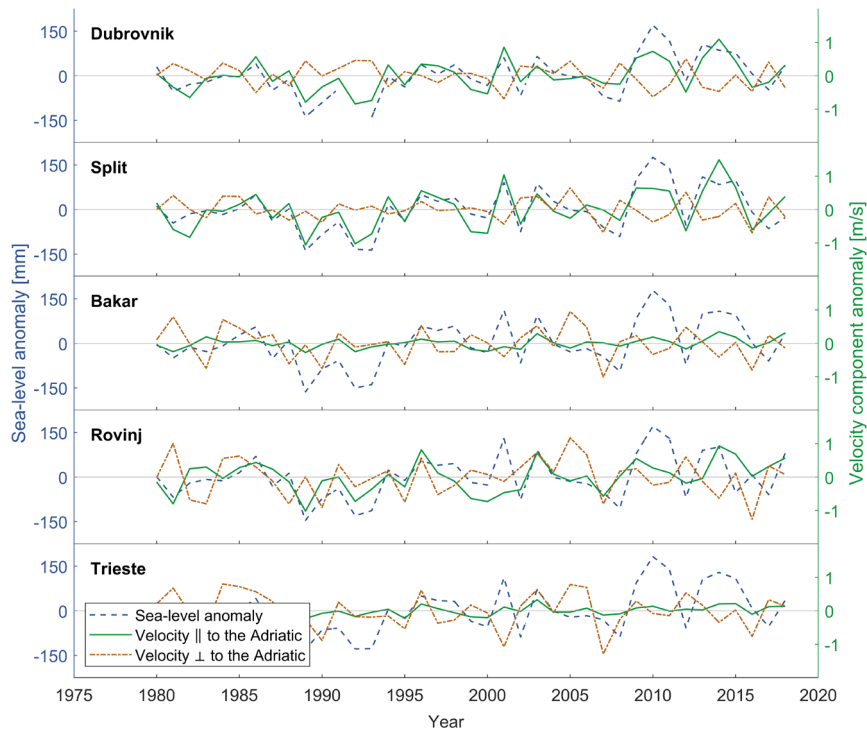


Figure 13. The annual mean NDJF season sea-level anomaly and wind data.

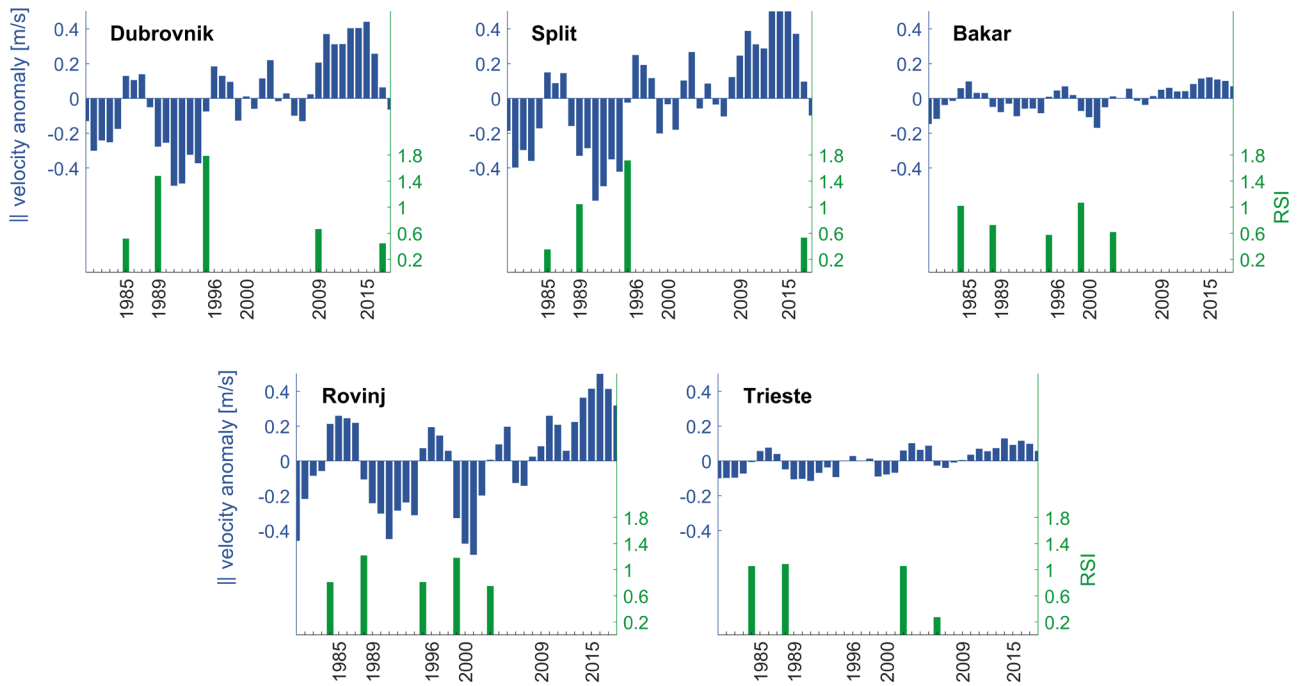


Figure 14. Parallel wind component regime shifts for the NDJF season. The shifts were calculated for 4-year moving mean dataset.

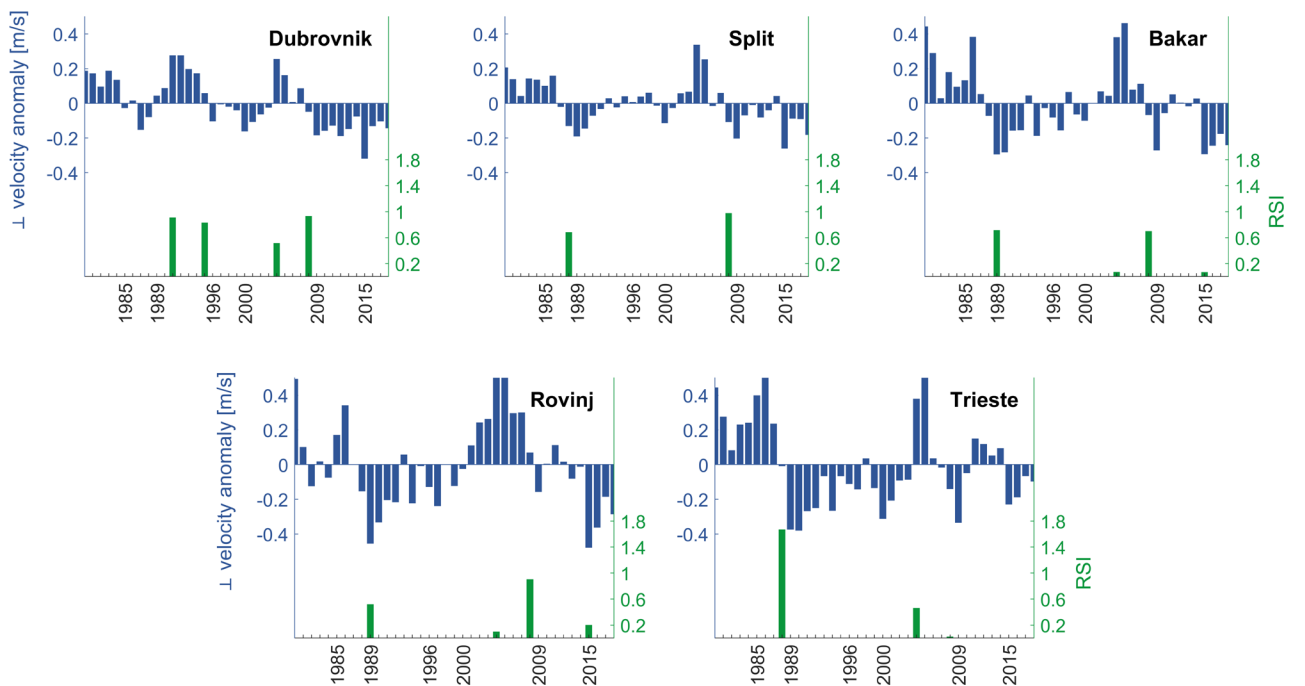


Figure 15. Orthogonal wind component regime shifts for the NDJF season. The shifts were calculated for 4-year moving mean dataset.

4.3. Synoptic Conditions Analysis

As presented in the earlier chapters, the NAO index, mean sea-level pressure and parallel wind component, are moderately to highly correlated to the sea-level variability in the Adriatic. On top of that, similar regime shifts were found for all data. Therefore, an overview of the synoptic conditions is given for the NDJF season for years of the most relevant regime shifts and the entire regimes as well. Upon individually evaluating the years of regime shifts, the NDJF season of 1988/1989, 1995/1996, and 2009/2010 transition years were chosen as indicators of synoptic conditions responsible for the regime change.

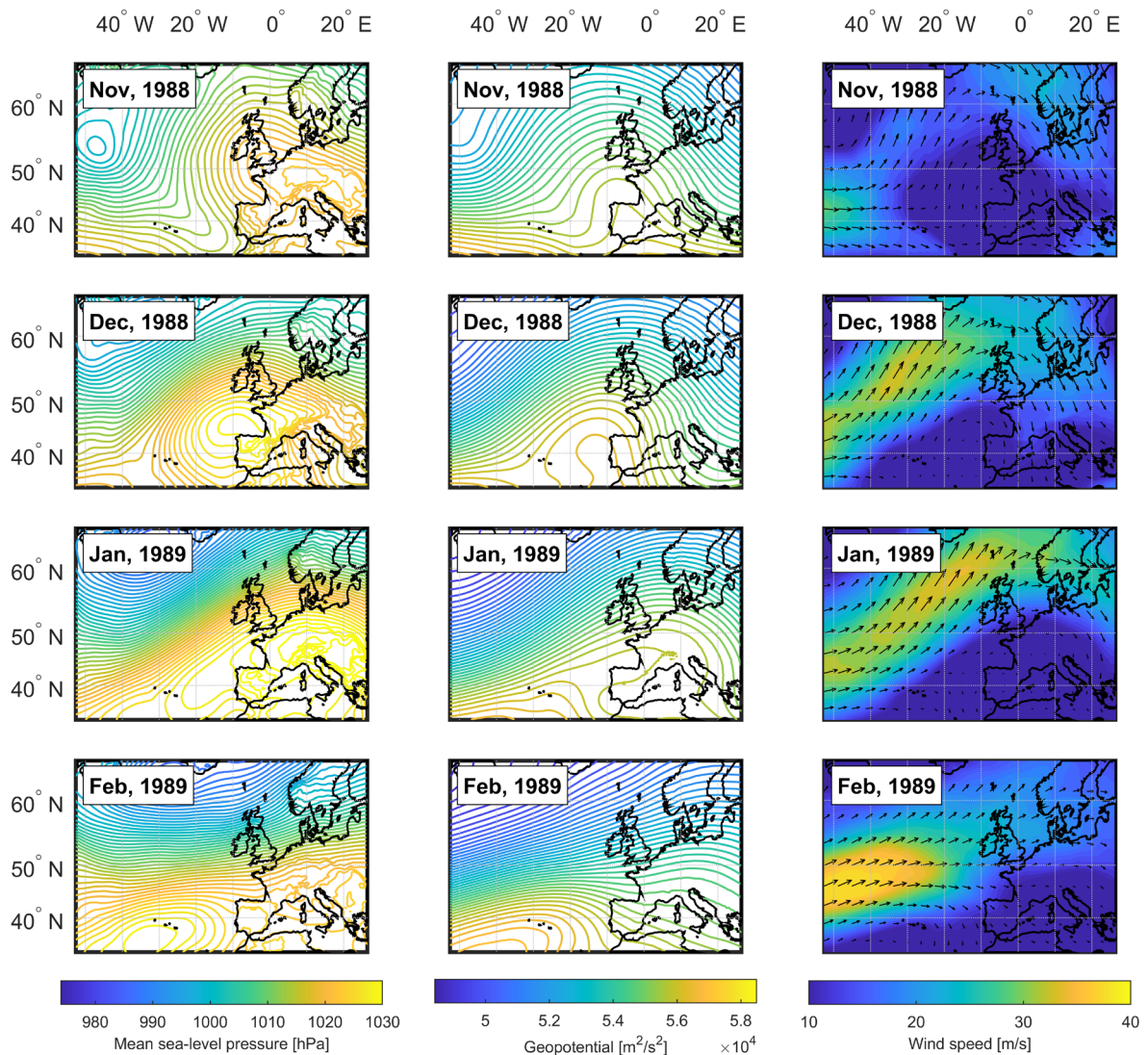


Figure 16. The NDJF season synoptic conditions for the 1988/1989 transition period. *Left panel:* mean sea-level pressure. *Middle panel:* geopotential at 500 hPa. *Right panel:* wind field at 500 hPa.

Figure 16 displays the synoptic conditions of the 1988/1989 NDJF transition period. The mean sea-level pressure data clearly displays a high-pressure field extending through the Mediterranean up to the British Isles, and a strong low-pressure field descending from Iceland. The 500 hPa geopotential and wind fields point to the jet stream channelling storms between the strong North Atlantic pressure systems towards Northern Europe leaving the Mediterranean dry. These conditions clearly correspond to the positive NAO phase, resulting in lower sea level across the Adriatic. The conditions were most pronounced for January 1989 when the mean sea-level pressure data over the Mediterranean surpassed 1030 hPa.

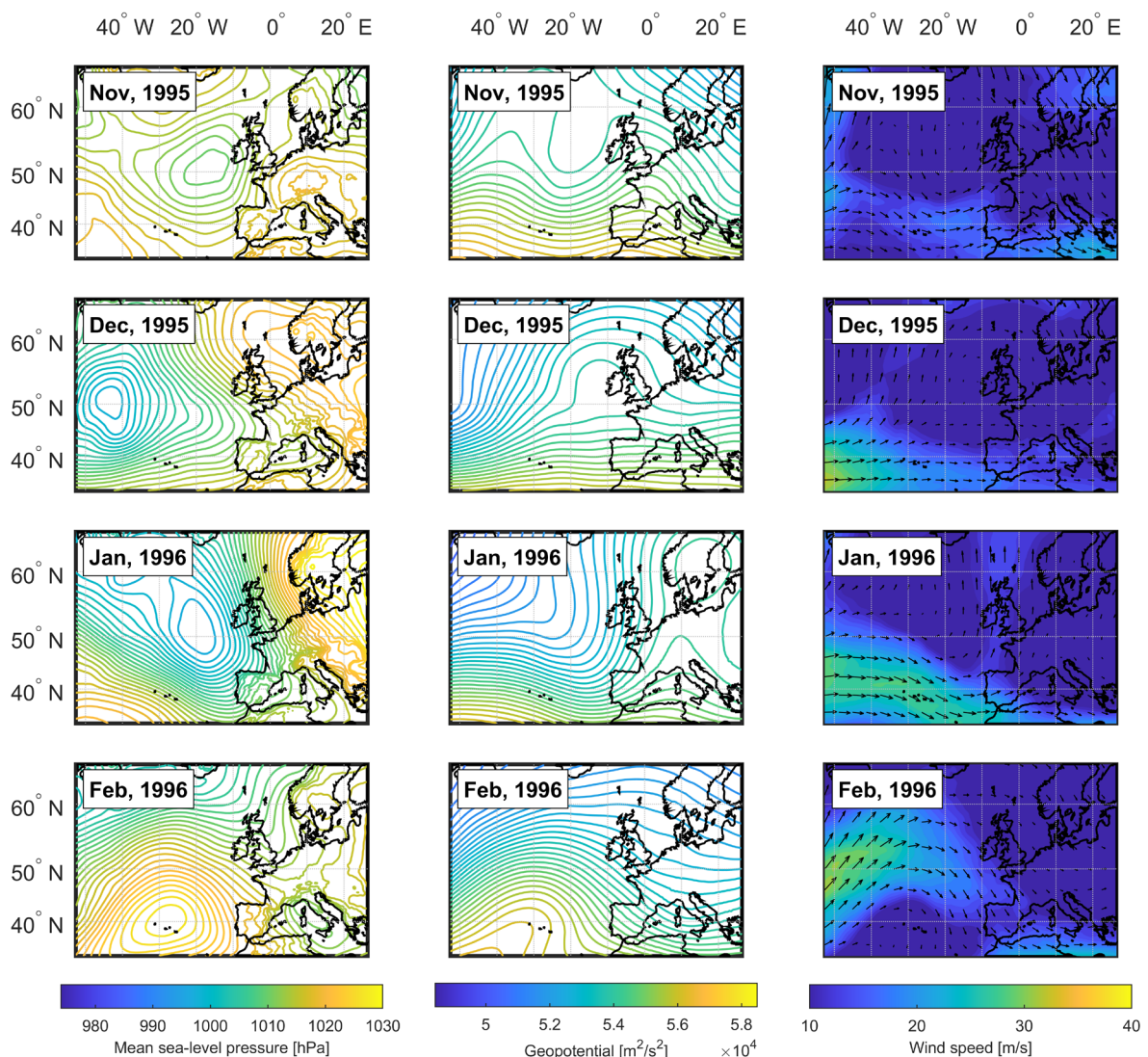


Figure 17. The NDJF season synoptic conditions for the 1995/1996 transition period. *Left panel:* mean sea-level pressure. *Middle panel:* geopotential at 500 hPa. *Right panel:* wind field at 500 hPa.

The 1995/1996 NDJF transition period was found to relate to the decrease in the NAO index, leading to synoptic conditions presented in Figure 17. In contrast to the 1988/1989 shift, the mean sea-level pressure data this time reached only about 1015 hPa across the Mediterranean since the Azores High is weaker and the Icelandic Low extends all the way to Western Europe. Moreover, this caused the Siberian High to be drawn into Northern Europe resulting in dry, cold air over that area. The 500 hPa geopotential and wind fields point that the jet stream bypassed the weak Icelandic Low and turned south channelling cyclonic activity to the Mediterranean. Consequently, it was shown that this correlates to higher sea levels across the Adriatic.

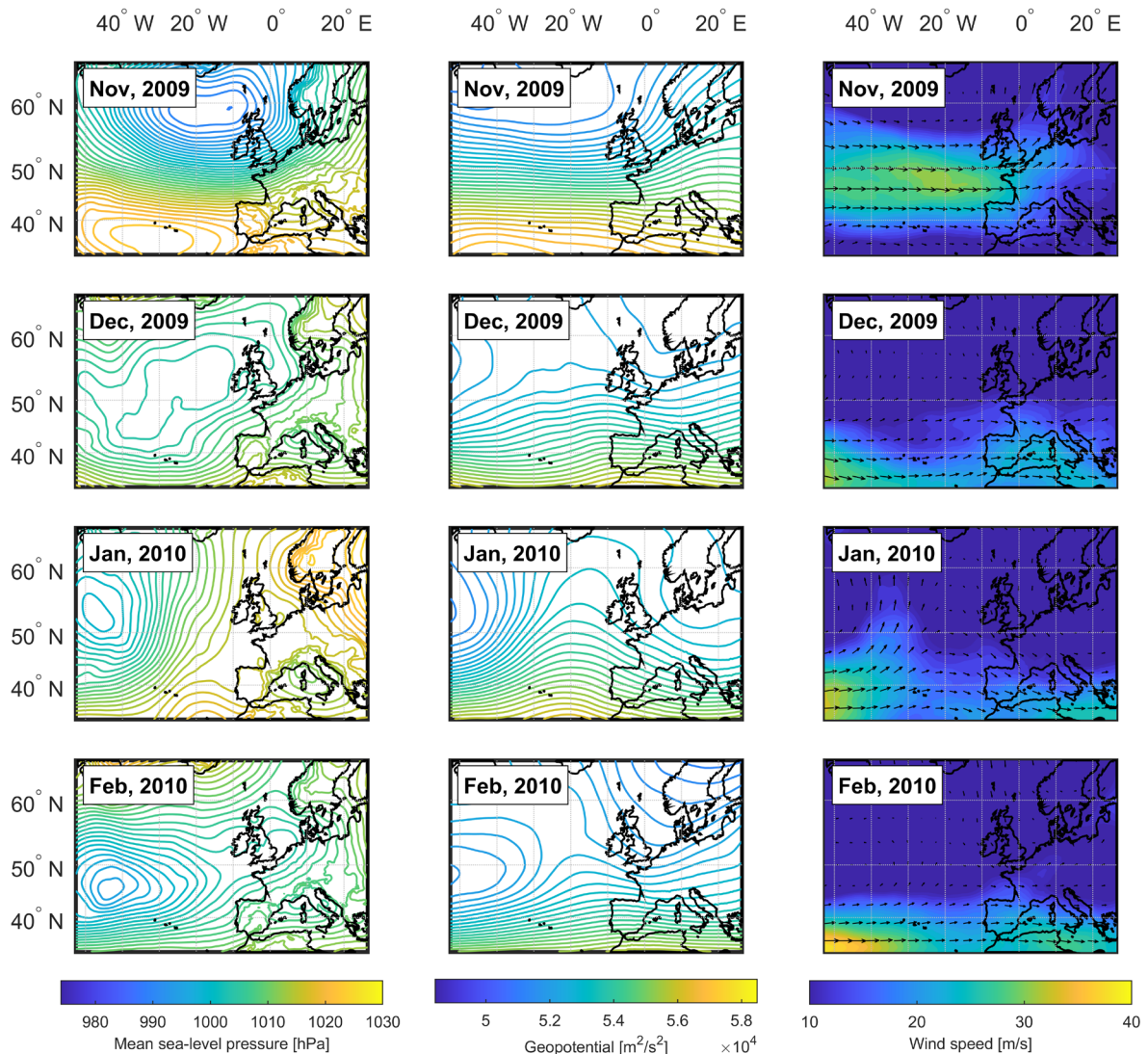


Figure 18. The NDJF season synoptic conditions for the 2009/2010 transition period. *Left panel:* mean sea-level pressure. *Middle panel:* geopotential at 500 hPa. *Right panel:* wind field at 500 hPa.

The last transition period resulting in a sea-level regime shift was found for the 2009/2010 NDJF season. The synoptic conditions are presented in Figure 18. This period's conditions were similar to the 1995/1996 situation since they also corresponded to the negative NAO index and increase of sea level across the Adriatic. Somewhat weaker Siberian High could be observed in Northern Europe and the low-pressure field once again extended further south than in the case of the 1988/1989 transition period, covering almost the entire domain in December 2009 and February 2010. The 500 hPa geopotential and wind fields show that the jet stream in the very south of the domain channelled cyclonic activity to the Mediterranean. Therefore, the 2009/2010 transition period displayed a stronger NAO negative phase and higher sea levels than the 1995/1996 transition period as found in prior analysis.

To analyse the conditions throughout the regimes, the mean sea-level pressure, 500 hPa geopotential and wind were averaged for the NDJF season for years 1989, 1990, 1992, and 1993 for the first regime; 1997, 1999, 2001, and 2004 for the second regime; and 2010, 2011, 2013, and 2015 for the third regime. Four years were chosen to represent each of the shifts after manually inspecting the conditions for every year.

The first found regime shift started in 1989 and it is a good representation of the positive phase of the North Atlantic Oscillation. The averaged mean sea-level pressure, geopotential, and wind data display the same characteristics found for the starting point of the shift. The pressure gradient and wind speed were fairly weaker, but the strong high-pressure and low-pressure systems are easily distinguished. The jet stream again conveyed storms between the pressure systems towards Northern Europe resulting in less cyclonic activity across the Mediterranean. This implies that the NAO index was predominantly positive during the 1989-1996 regime, which agrees with the prior analysis. The result is shown in Figure 19.

The next regime shift started with a sharp drop of the NAO index in 1996 and lasted until 2009 (Figure 20). However, during these years, the NAO index was slightly positive in 1999, 2000, 2002, 2003, 2004, and 2007. The result displays weaker mean sea-level pressure systems and weaker pressure gradient, but when compared to the first regime, the mean sea-level pressure over the Adriatic was only slightly lower. However, because of the weaker gradient, the 500 hPa geopotential and wind fields show the jet stream was channelling cyclonic activity in the very south of the domain, over the Mediterranean. It was shown that this resulted in higher sea levels across the Adriatic for an average of 2.07 cm.

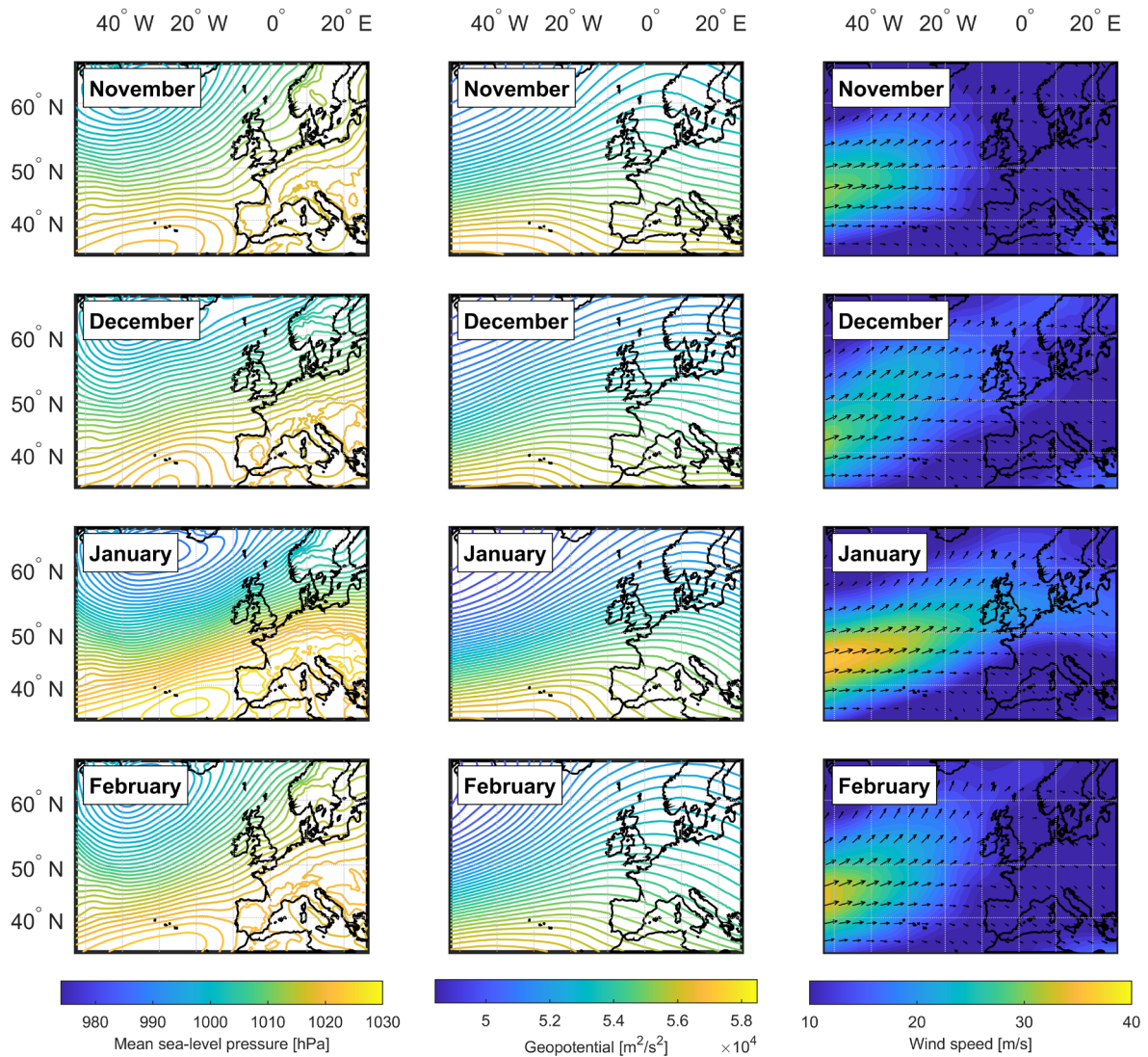


Figure 19. The annual mean NDJF season synoptic conditions for the 1989-1996 regime. *Left panel:* mean sea-level pressure. *Middle panel:* geopotential at 500 hPa. *Right panel:* wind field at 500 hPa.

The last regime shift started in 2009 and has been active at least until 2018. The synoptic conditions overview presented in Figure 21 once more show weak high-pressure and low-pressure systems, with low gradient in-between. The resulting jet stream was therefore weaker, and the westerlies were moved southward, bringing warm moist air over the Mediterranean. This indicates the NAO was on average in its negative phase during this last sea-level shift, even though it had some positive values from year 2013 until 2018.

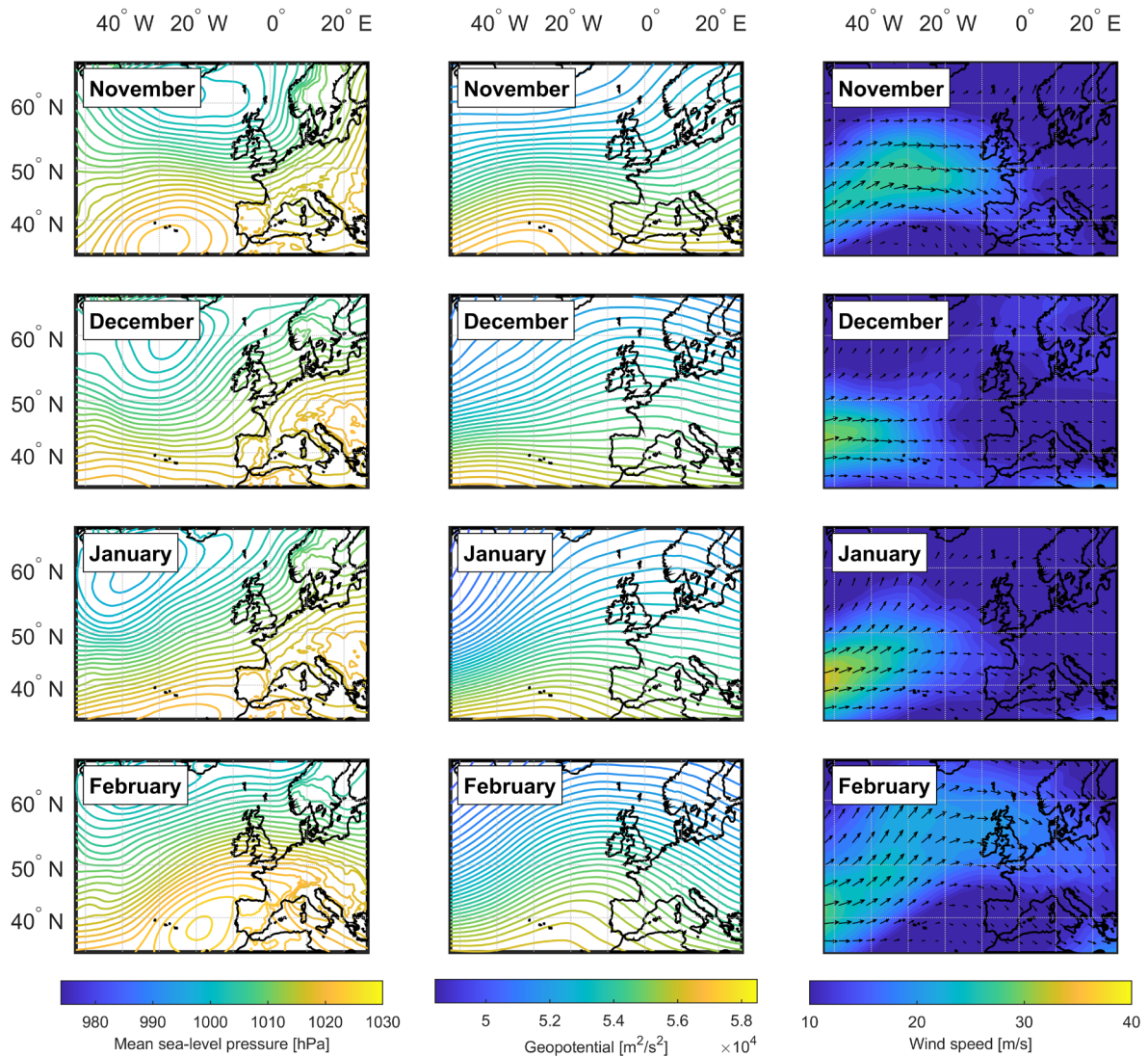


Figure 20. The annual mean NDJF season synoptic conditions for the 1996-2009 regime. *Left panel:* mean sea-level pressure. *Middle panel:* geopotential at 500 hPa. *Right panel:* wind field at 500 hPa.

To conclude, the synoptic analysis demonstrated that all climatic shifts were related to pronounced changes of the NAO. When comparing Figure 19 to Figure 20 and Figure 21, the different effects that the NAO generated across the Mediterranean, and thus Adriatic, are evident. The positive phase in 1989-1996 likely corresponded to less cyclonic activity over the Mediterranean, while the negative phases from 1996-2009, and 2009-2018 corresponded to higher cyclonic activity. It is important to note that the negative phases are not the only cause of sea-level rise, as the climate change should also be considered.

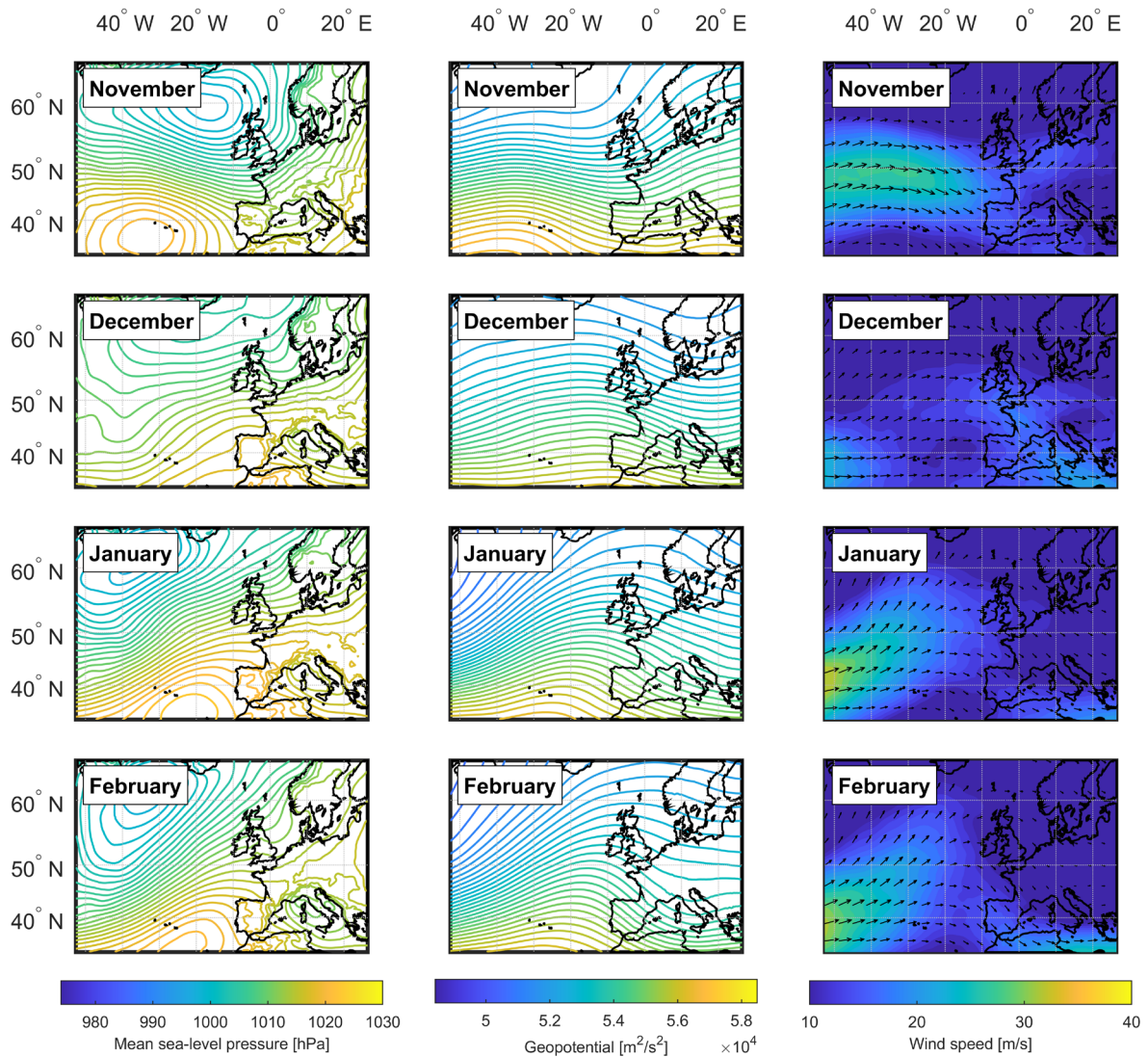


Figure 21. The annual mean NDJF season synoptic conditions for the 2009-present regime. *Left panel:* mean sea-level pressure. *Middle panel:* geopotential at 500 hPa. *Right panel:* wind field at 500 hPa.

4.3.1. Mean Sea-level Pressure Over The Adriatic Sea

To better understand the sea-level regime shifts over the Adriatic, the mean-sea level pressure synoptic fields over the Adriatic were further analysed. The analysis was done for the NDJF season 1988/1989, 1995/1996, and 2009/2010 transition periods.

The NDJF season mean sea-level pressure fields over the Adriatic for the 1988/1989 transition period are presented in Figure 22. The result shows mean sea-level pressure ranged

from about 1020 hPa to about 1032 hPa. The minimum values were obtained for November and December 1988, while the maximum values were obtained for January 1989.

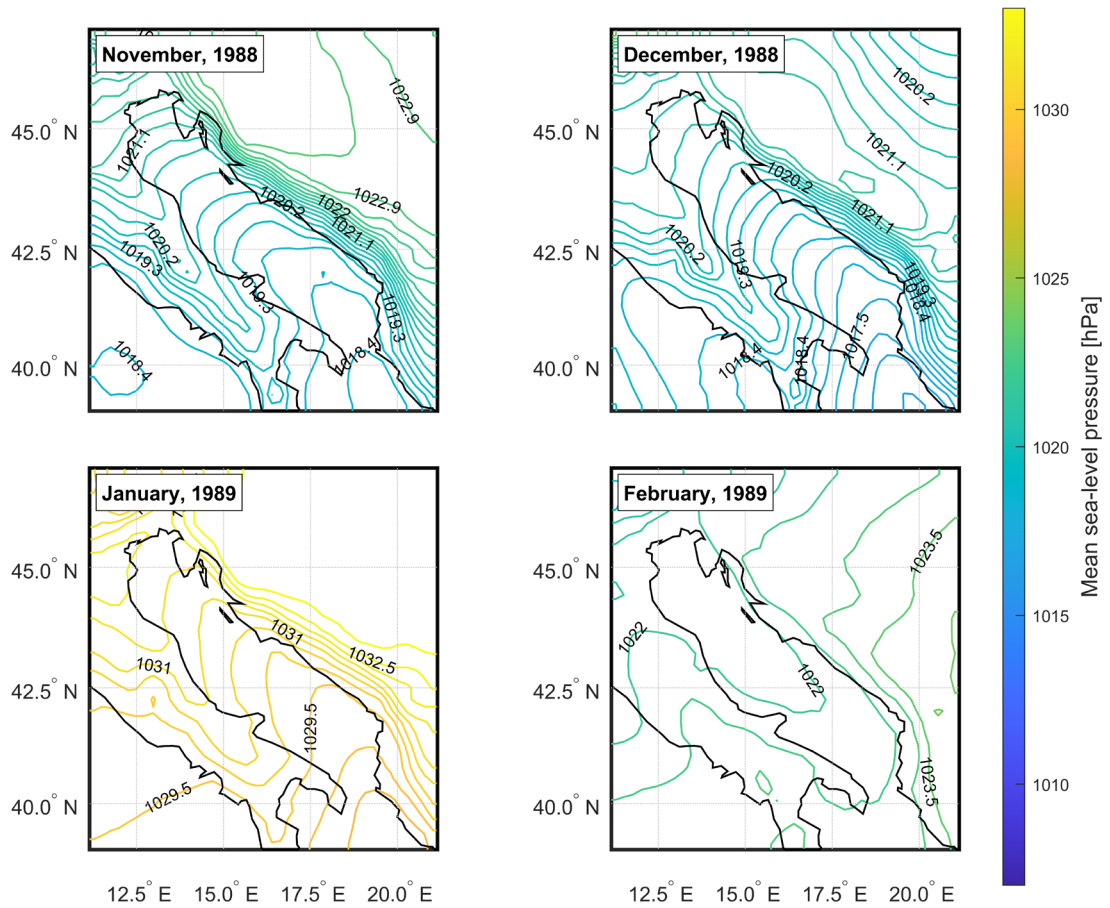


Figure 22. The NDJF season mean sea-level pressure fields over the Adriatic Sea for the 1988/1989 transition period.

Next, the same analysis was done for positive regime shifts: the 1995/1996 and 2009/2010 transition periods. For the 1995/1996 transition period, the mean sea-level pressure values ranged from about 1011 hPa to approximately 1017 hPa, as seen from Figure 23. The minimum values were obtained for February 1996, while the maxima were obtained for November 1995. For the 2009/2010 transition, however, the values ranged from about 1007 hPa to about 1016 hPa, with the maxima in November 2009, and minima in February 2010. The NDJF 2009/2010 transition period mean sea-level pressure fields over the Adriatic are presented in Figure 24.

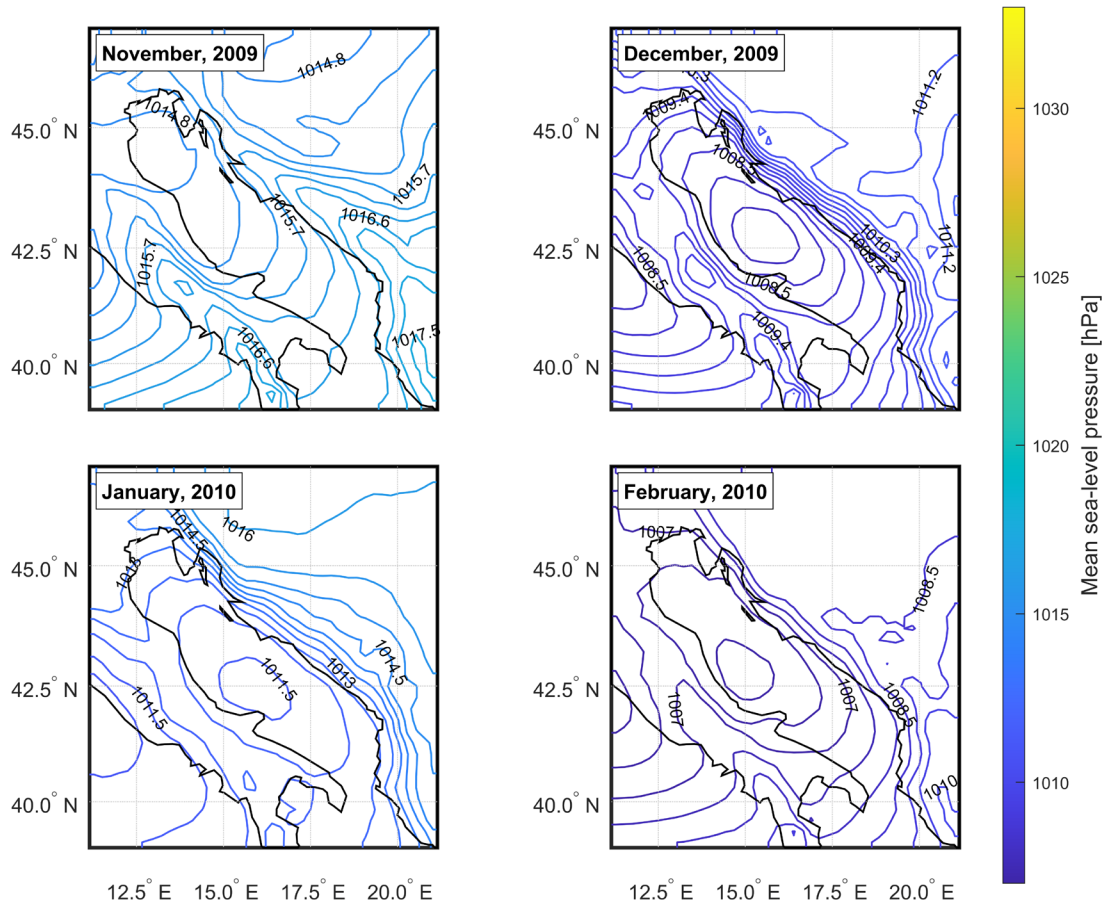


Figure 24. The NDJF season mean sea-level pressure over the Adriatic Sea for the 2009/2010 transition period.

5. Conclusion

In this study, an analysis of the observed Adriatic mean sea-level time series has been carried out in order to determine the primary causes of the changes documented during the last 50 years. Significant positive sea-level trend, related to climate change, was detected for all stations. Further on, using Rodionov's regime shift index algorithm, several regime shifts were detected. The first pronounced regime shift occurred in 1989 resulting with mean sea level lower than usual for an average of 4.37 cm during the next 7 years; the second regime shift occurred in 1996 when mean sea level increased for an average of 2.07 cm during the next 13 years; and the third regime shift, which lasted at least until 2018, started in 2009 when mean sea level abruptly increased to 5.3 cm above average during the 2009-2018 period.

A relationship between the North Atlantic Oscillation (NAO) and sea-level data has been explored establishing moderate and statistically significant correlation between the two for all data, and even stronger correlation for the November-December-January-February (NDJF) season. All climate shifts were related to pronounced changes of the NAO. The negative shift starting in 1989 was related to the positive phase of the NAO, i.e. to weaker cyclonic activity over the Mediterranean and the Adriatic Sea. Oppositely, the two latter positive regime shifts were related to significant decrease and negative phases of the NAO, with the NAO reaching the most negative values of the entire observation period during the shift starting in 2009. Negative phase of the NAO corresponds to stronger cyclonic activity over the Mediterranean and the Adriatic Sea.

Furthermore, since the NAO influence on the Mediterranean sea level is primarily manifested by the local atmospheric pressure effects and wind field over the basin, the mean sea-level pressure and wind data were further analysed. It was shown that the mean sea-level pressure and the longshore wind were highly correlated to the recorded sea-level change. The former is because of the inverse barometer effect, which explained up to 49% of sea-level variability for the NDJF season, while the latter is presumed to be because of the Ekman transport and building up of water due to the sirocco wind, but it lacks detailed analysis. Moreover, regime shifts similar to the ones for sea level data were detected for all climatic atmospheric data.

Lastly, observed regime shifts were further analysed by reviewing synoptic conditions. It was once more confirmed that all the climate shifts were related to pronounced changes of the NAO.

In conclusion, the documented variability of the Adriatic sea level during the last 50 years, and in particular the accelerated rise during the last 20 years, represent a combination of mean sea-level rise due to climate change and due to atmospherically induced shift of climate regimes, which are manifested by the local atmospheric pressure and wind field variability.

Literature

- [1] IPCC, 2021: Summary for Policymakers. In: *Climate Change 2021: The Physical Science Basis. Contribution of Working Group I to the Sixth Assessment Report of the Intergovernmental Panel on Climate Change* [MASSON-DELMOTTE, V., P. ZHAI, A. PIRANI, S.L.CONNORS, C. PÉAN, S. BERGER, N. CAUD, Y. CHEN, L. GOLDFARB, M.I. GOMIS, M. HUANG, K. LEITZELL, E. LONNOY, J.B.R. MATTHEWS, T.K. MAYCOCK, T. WATERFIELD, O. YELEKÇI, R. YU, AND B. ZHOU (EDS.)]. IN PRESS.
- [2] MIMURA, N., 2013. *Sea-level rise caused by climate change and its implications for society*. Proceedings of the Japan Academy, Series B Physical and Biological Sciences, 89(7): 281–301.
- [3] CUSHMAN-ROISIN B., GAČIĆ M., POULAIN P.M., ARTEGIANI A., 2001. *Physical Oceanography of the Adriatic Sea: Past, Present and Future*. Springer-Science + Business Media, B.V. DOI: 10.1007/978-94-015-9819-4
- [4] ORLIĆ, M., KUZMIĆ, M., AND PASARIĆ, Z., 1994. *Response of the Adriatic Sea to the bora and sirocco forcing*. *Continental Shelf Research*, 14(1), 91–116. DOI:10.1016/0278-4343(94)90007-8
- [5] CHURCH, J.A., P.U. CLARK, A. CAZENAVE, J.M. GREGORY, S. JEVREJEVA, A. LEVERMANN, M.A. MERRIFIELD, G.A. MILNE, R.S. NEREM, P.D. NUNN, A.J. PAYNE, W.T. PFEFFER, D. STAMMER AND A.S. UNNIKRIISHNAN, 2013: *Sea Level Change*. In: *Climate Change 2013: The Physical Science Basis. Contribution of Working Group I to the Fifth Assessment Report of the Intergovernmental Panel on Climate Change* [STOCKER, T.F., D. QIN, G.-K. PLATTNER, M. TIGNOR, S.K. ALLEN, J. BOSCHUNG, A. NAUELS, Y. XIA, V. BEX AND P.M. MIDGLEY (EDS.)]. Cambridge University Press, Cambridge, United Kingdom and New York, NY, USA
- [6] VILIBIĆ, I., ŠEPIĆ, J., PASARIĆ, M., & ORLIĆ, M., 2017. *The Adriatic Sea: A Long-Standing Laboratory for Sea Level Studies*. *Pure and Applied Geophysics*, 174(10), 3765–3811. DOI:10.1007/s00024-017-1625-8
- [7] RAFFERTY, J. P., 2011. *North Atlantic Oscillation*. *Encyclopedia Britannica*, <https://www.britannica.com/science/North-Atlantic-Oscillation>, Accessed 28 February 2022.

- [8] URL: <https://www.ncei.noaa.gov/access/monitoring/nao/>, Accessed 20 September 2022
- [9] URL: <https://cds.climate.copernicus.eu/cdsapp#!/dataset/reanalysis-era5-single-levels?tab=overview>, Accessed 20 September 2022
- [10] CALAFAT, F. M., D. P. CHAMBERS, AND M. N. TSIMPLIS, 2012. *Mechanisms of decadal sea level variability in the eastern North Atlantic and the Mediterranean Sea*, Journal of Geophysical Research, 117, C09022, DOI:10.1029/2012JC008285.
- [11] URL: <https://www.investopedia.com/terms/l/least-squares-method.asp>, Accessed 6 September 2022.
- [12] URL: <https://www.investopedia.com/terms/t/t-test.asp>, Accessed 6 September 2022.
- [13] RODIONOV, S. N., 2004. *A sequential algorithm for testing climate regime shifts*, Geophysical Research Letters, 31, L09204, DOI:10.1029/2004GL019448.
- [14] URL: <https://uk.mathworks.com/help/matlab/ref/corrcoef.html>, Accessed 24 September 2022.

List of Figures

Figure 1. The negative and positive NAO phase. The strength and direction of westerlies and location of storm tracks are controlled by strength of Azores High and Iceland Low. The figure was made by the author using MATLAB R2021b and Inkscape software..... 4

Figure 2. Location of tide gauge stations used in the study..... 5

Figure 3. The annual mean sea-level anomaly for seven stations across the Adriatic coast. 11

Figure 4. The annual mean sea-level data with denoted possible regimes and their means. 12

Figure 5. The annual mean sea-level data and linear trend estimated for seven stations across the Adriatic coast. Linear equations are given for each computed trend. 13

Figure 6. Regime shifts of sea levels. The upper graph displays the annual mean sea-level anomaly, while the lower graph displays the computed regime shifts. Bar plots are used for easier visualization. Three regime shifts can be detected for almost every station: in 1989, in 1996, and in 2009. 14

Figure 7. The NAO index and sea-level annual (left) and 4-year moving (right) means. The positive NAO index (green) corresponds to lower sea levels (dashed blue)..... 16

Figure 8. The NAO index and sea level Nov-Dec-Jan-Feb season annual means. The positive NAO index (green) corresponds to lower sea levels (dashed blue)..... 17

Figure 9. The NAO index regime shifts in case of a 4-year moving mean (left) and Nov-Dec-Jan-Feb season 4-year moving mean (right). Multiple regime shifts were detected, including the shifts around the years of interest: 1989, 1996, and 2009. 18

Figure 10. Sea level (dashed blue) and mean sea-level pressure anomaly (green) NDJF season annual means. The mean sea-level pressure data was multiplied by -1 for easier interpretation of correlation. 19

Figure 11. Sea-level anomaly and the IB effect of the complete data set (left) and the NDJF season (right). Both time series were smoothed using a 4-year moving mean. 20

| | |
|--|----|
| Figure 12. Mean sea-level pressure regime shifts for the NDJF season. The shifts were calculated for 4-year moving mean dataset. Four regime shifts can be detected for all data: in 1989, 1995, 2010, and in 2016. | 21 |
| Figure 13. The annual mean NDJF season sea-level anomaly and wind data..... | 22 |
| Figure 14. Parallel wind component regime shifts for the NDJF season. The shifts were calculated for 4-year moving mean dataset. | 23 |
| Figure 15. Orthogonal wind component regime shifts for the NDJF season. The shifts were calculated for 4-year moving mean dataset. | 23 |
| Figure 16. The NDJF season synoptic conditions for the 1988/1989 transition period. <i>Left panel:</i> mean sea-level pressure. <i>Middle panel:</i> geopotential at 500 hPa. <i>Right panel:</i> wind field at 500 hPa. | 24 |
| Figure 17. The NDJF season synoptic conditions for the 1995/1996 transition period. <i>Left panel:</i> mean sea-level pressure. <i>Middle panel:</i> geopotential at 500 hPa. <i>Right panel:</i> wind field at 500 hPa. | 25 |
| Figure 18. The NDJF season synoptic conditions for the 2009/2010 transition period. <i>Left panel:</i> mean sea-level pressure. <i>Middle panel:</i> geopotential at 500 hPa. <i>Right panel:</i> wind field at 500 hPa. | 26 |
| Figure 19. The annual mean NDJF season synoptic conditions for the 1989-1996 regime. <i>Left panel:</i> mean sea-level pressure. <i>Middle panel:</i> geopotential at 500 hPa. <i>Right panel:</i> wind field at 500 hPa. | 28 |
| Figure 20. The annual mean NDJF season synoptic conditions for the 1996-2009 regime. <i>Left panel:</i> mean sea-level pressure. <i>Middle panel:</i> geopotential at 500 hPa. <i>Right panel:</i> wind field at 500 hPa. | 29 |
| Figure 21. The annual mean NDJF season synoptic conditions for the 2009-present regime. <i>Left panel:</i> mean sea-level pressure. <i>Middle panel:</i> geopotential at 500 hPa. <i>Right panel:</i> wind field at 500 hPa. | 30 |
| Figure 22. The NDJF season mean sea-level pressure fields over the Adriatic Sea for the 1988/1989 transition period..... | 31 |
| Figure 23. The NDJF season mean sea-level pressure fields over the Adriatic Sea for the 1995/1996 transition period..... | 32 |

| | |
|--|----|
| Figure 24. The NDJF season mean sea-level pressure over the Adriatic Sea for the 2009/2010 transition period..... | 33 |
|--|----|

List of Tables

| | |
|--|----|
| Table 1. Student’s t-test results..... | 13 |
| Table 2. The NAO index and sea level correlation with corresponding p-value..... | 15 |
| Table 3. The NAO index and sea level correlation with p-value for the DJFM and NDJF season. | 17 |
| Table 4. Mean sea-level pressure and sea-level data NDJF season annual and 4-year moving mean correlation with corresponding p-value. | 19 |
| Table 5. Correlation coefficients and its p-value for the parallel (\parallel) wind component and the orthogonal (\perp) wind component and sea-level data. The NDJF season annual means were used..... | 22 |

Appendix A

Once we find the t-value of a t-test, and calculate the degrees of freedom (DF), we can compare the t-value to the critical value from the cumulative t-distribution table for one-tail P = 0.05 (third column).

| | P | | | | | | |
|-----------|-------|-------|--------|--------|--------|---------|---------|
| one-tail | 0.1 | 0.05 | 0.025 | 0.01 | 0.005 | 0.001 | 0.0005 |
| two-tails | 0.2 | 0.1 | 0.05 | 0.02 | 0.01 | 0.002 | 0.001 |
| DF | | | | | | | |
| 1 | 3.078 | 6.314 | 12.706 | 31.821 | 63.656 | 318.289 | 636.578 |
| 2 | 1.886 | 2.92 | 4.303 | 6.965 | 9.925 | 22.328 | 31.6 |
| 3 | 1.638 | 2.353 | 3.182 | 4.541 | 5.841 | 10.214 | 12.924 |
| 4 | 1.533 | 2.132 | 2.776 | 3.747 | 4.604 | 7.173 | 8.61 |
| 5 | 1.476 | 2.015 | 2.571 | 3.365 | 4.032 | 5.894 | 6.869 |
| 6 | 1.44 | 1.943 | 2.447 | 3.143 | 3.707 | 5.208 | 5.959 |
| 7 | 1.415 | 1.895 | 2.365 | 2.998 | 3.499 | 4.785 | 5.408 |
| 8 | 1.397 | 1.86 | 2.306 | 2.896 | 3.355 | 4.501 | 5.041 |
| 9 | 1.383 | 1.833 | 2.262 | 2.821 | 3.25 | 4.297 | 4.781 |
| 10 | 1.372 | 1.812 | 2.228 | 2.764 | 3.169 | 4.144 | 4.587 |
| 11 | 1.363 | 1.796 | 2.201 | 2.718 | 3.106 | 4.025 | 4.437 |
| 12 | 1.356 | 1.782 | 2.179 | 2.681 | 3.055 | 3.93 | 4.318 |
| 13 | 1.35 | 1.771 | 2.16 | 2.65 | 3.012 | 3.852 | 4.221 |
| 14 | 1.345 | 1.761 | 2.145 | 2.624 | 2.977 | 3.787 | 4.14 |
| 15 | 1.341 | 1.753 | 2.131 | 2.602 | 2.947 | 3.733 | 4.073 |
| 16 | 1.337 | 1.746 | 2.12 | 2.583 | 2.921 | 3.686 | 4.015 |
| 17 | 1.333 | 1.74 | 2.11 | 2.567 | 2.898 | 3.646 | 3.965 |
| 18 | 1.33 | 1.734 | 2.101 | 2.552 | 2.878 | 3.61 | 3.922 |
| 19 | 1.328 | 1.729 | 2.093 | 2.539 | 2.861 | 3.579 | 3.883 |
| 20 | 1.325 | 1.725 | 2.086 | 2.528 | 2.845 | 3.552 | 3.85 |
| 21 | 1.323 | 1.721 | 2.08 | 2.518 | 2.831 | 3.527 | 3.819 |
| 22 | 1.321 | 1.717 | 2.074 | 2.508 | 2.819 | 3.505 | 3.792 |
| 23 | 1.319 | 1.714 | 2.069 | 2.5 | 2.807 | 3.485 | 3.768 |
| 24 | 1.318 | 1.711 | 2.064 | 2.492 | 2.797 | 3.467 | 3.745 |
| 25 | 1.316 | 1.708 | 2.06 | 2.485 | 2.787 | 3.45 | 3.725 |
| 26 | 1.315 | 1.706 | 2.056 | 2.479 | 2.779 | 3.435 | 3.707 |
| 27 | 1.314 | 1.703 | 2.052 | 2.473 | 2.771 | 3.421 | 3.689 |
| 28 | 1.313 | 1.701 | 2.048 | 2.467 | 2.763 | 3.408 | 3.674 |
| 29 | 1.311 | 1.699 | 2.045 | 2.462 | 2.756 | 3.396 | 3.66 |
| 30 | 1.31 | 1.697 | 2.042 | 2.457 | 2.75 | 3.385 | 3.646 |
| 60 | 1.296 | 1.671 | 2 | 2.39 | 2.66 | 3.232 | 3.46 |
| 120 | 1.289 | 1.658 | 1.98 | 2.358 | 2.617 | 3.16 | 3.373 |
| 1000 | 1.282 | 1.646 | 1.962 | 2.33 | 2.581 | 3.098 | 3.3 |
| Inf | 1.282 | 1.645 | 1.96 | 2.326 | 2.576 | 3.091 | 3.291 |

Appendix B

```
function [RSI,xtemp,shift] = Rodionov(X,t,L)

% Example:
% i = 3; % Split
% [RSI,xtemp,shift] = Rodionov(sl.(stations{i}),2.1,10);

% variables
    len = length(X);
    shift = []; % shift points
    changepoint = 1;

% average st.dev (variance when squared) for running
% 1-year intervals in time series of variable X
    var_L = mean(movvar(X,L,'Endpoints','discard'));

% diff is the difference between mean values of two
% subsequent regimes that would be statistically
% significant according to the Student's t-test
    diff = t * sqrt(2 * var_L / L);

% initial, first regime, R1, mean value
    x1 = mean(X(1:L));

%% loop
for j = L+1 : len

    % reset for new loop iteration
    xtemp = zeros(1,len);

    % regime doesn't change:
    if abs(X(j) - x1) <= diff
        if (j-(L-1)) > changepoint
            x1 = mean(X(j-(L-1):j));
        end
        continue

    % possible regime changes:
    else
        for i = j : j+L-1
            if i > len
                break;
            else
                if (X(j) > (x1 + diff)) == true % keeps calc the same eq
                    xtemp(i) = X(i) - (x1 + diff);
                else
                    xtemp(i) = (x1 - diff) - X(i);
                end
            end
            RSI(j) = sum(xtemp) / (L * sqrt(var_L)); %
            if RSI(j) <= 0
                RSI(j) = 0;
                x1 = mean(X(j-L+1:j));
                break;
            end
        end
    end
end
```

```
        end
    end
end

% recording the shift
if RSI(j) > 0
    shift = [shift, j];
    changepoint = max(shift);
    if (j+L-1) > len
        x1 = mean(X(j:end));
    else
        x1 = mean(X(j:j+L-1));
    end
end
end

end

end
```